

AD-A208 436

DTIC FILE COPY

①

HIGH PERFORMANCE COMPOSITES BASED ON POLYURETHANES REINFORCED WITH
POLYDIACETYLENES

UNITED STATES ARMY - UMIST

Final Report
Results of Research and Development work
undertaken at UMIST,
December 1986-December 1987

John L. Stanford and Robert J. Young

Polymer Science and Technology Group, Manchester Materials Science Centre,
UMIST, P.O. Box 88, Manchester, M60 1QD, UK.

United States Army, U.S.A.R.D.S.G. - UK

Contract Number DAJA45-86-C-0058 *Unrestricted*

The research reported in this document is based on experimental work carried out by a Research Assistant, Ahmad K. Dard, and was made possible through the support and sponsorship of the US Government through its European Research Office of the US Army. ~~This report is intended only for the internal management use of the Contractor and the US Government.~~

DTIC
ELECTE
MAY 19 1989
S H D

DISTRIBUTION STATEMENT A

Approved for public release;
Distribution Unlimited

89 5 19 164

Unclassified
SECURITY CLASSIFICATION OF THIS PAGE

REPORT DOCUMENTATION PAGE				Form Approved OMB No 0704-0188 Exp. Date Jun 30, 1986	
1a. REPORT SECURITY CLASSIFICATION Unclassified		1b. RESTRICTIVE MARKINGS			
2a. SECURITY CLASSIFICATION AUTHORITY		3. DISTRIBUTION/AVAILABILITY OF REPORT Approved for public release; distribution unlimited			
2b. DECLASSIFICATION/DOWNGRADING SCHEDULE					
4. PERFORMING ORGANIZATION REPORT NUMBER(S)		5. MONITORING ORGANIZATION REPORT NUMBER(S) R&D 4858A-MS-01			
6a. NAME OF PERFORMING ORGANIZATION University of Manchester & UMIST		6b. OFFICE SYMBOL (If applicable)	7a. NAME OF MONITORING ORGANIZATION European Research Office USARDCG-UK		
6c. ADDRESS (City, State, and ZIP Code) Manchester Materials Science Centre Grosvenor Street Manchester, M1 7HS, UK		7b. ADDRESS (City, State, and ZIP Code) Box 65 FPO NY 09510-1500			
8a. NAME OF FUNDING / SPONSORING ORGANIZATION USARDCG-UK AR0-E		8b. OFFICE SYMBOL (If applicable)	9. PROCUREMENT INSTRUMENT IDENTIFICATION NUMBER DAJA45-86-C-0058		
8c. ADDRESS (City, State, and ZIP Code) Box 65 FPO NY 09510-1500		10. SOURCE OF FUNDING NUMBERS	PROGRAM ELEMENT NO. 61103A	PROJECT NO. 1L161103BH57	TASK NO. 04
				WORK UNIT ACCESSION NO	
11. TITLE (Include Security Classification) (U) High Performance Composites Based on Polyurethanes Reinforced with Polydiacetylenes					
12. PERSONAL AUTHOR(S) John L. Stanford and Robert J. Young					
13a. TYPE OF REPORT Final		13b. TIME COVERED FROM DEC 86 TO DEC 87	14. DATE OF REPORT (Year, Month, Day) 1989, April 4th		15. PAGE COUNT 61
16. SUPPLEMENTARY NOTATION					
17. COSATI CODES			18. SUBJECT TERMS (Continue on reverse if necessary and identify by block number)		
FIELD	GROUP	SUB-GROUP	Polyurethanes; polydiacetylenes; phase-separated copolymers; composites; Raman spectroscopy; deformation.		
11	04				
07	03				
19. ABSTRACT (Continue on reverse if necessary and identify by block number)					
<p>This final report covers all the work carried out during the period from December 1986 to December 1987, and is a much more extended and detailed version of the two Interim Reports for December 1986-January 1987 and February-May 1987. The scientific programme was concerned with the development of high-performance composites based on various linear and crosslinked polyurethane matrices reinforced with high-strength and high-stiffness polydiacetylenes, incorporated either as single crystal fibres or as dispersed hard segment domains. The report is therefore presented in two parts (I) and (II) entitled</p> <p>(I) Formation and Properties of Fibre-Reinforced Composites: Polyurethane Resins containing Polydiacetylene Single Crystal Fibres.</p>					
20. DISTRIBUTION/AVAILABILITY OF ABSTRACT <input checked="" type="checkbox"/> UNCLASSIFIED/UNLIMITED <input checked="" type="checkbox"/> SAME AS RPT. <input checked="" type="checkbox"/> DTIC USERS			21. ABSTRACT SECURITY CLASSIFICATION Unclassified		
22a. NAME OF RESPONSIBLE INDIVIDUAL Dr. Wilbur C. Simmons			22b. TELEPHONE (Include Area Code) 01-409 4423	22c. OFFICE SYMBOL AMXSN-UK-RM	

HIGH PERFORMANCE COMPOSITES BASED ON POLYURETHANES REINFORCED WITH
POLYDIACETYLENES

UNITED STATES ARMY - UMIST

Final Report
Results of Research and Development work
undertaken at UMIST,
December 1986-December 1987

John L. Stanford and Robert J. Young

Polymer Science and Technology Group, Manchester Materials Science Centre,
UMIST, P.O. Box 88, Manchester, M60 1QD, UK.

United States Army, U.S.A.R.D.S.G. - UK

Contract Number DAJA45-86-C-0058

The research reported in this document is based on experimental work carried out by a Research Assistant, Ahmad K. Dard, and was made possible through the support and sponsorship of the US Government through its European Research Office of the US Army. This report is intended only for the internal management use of the Contractor and the US Government.

CONTENTS

	Page
<u>SUMMARY</u>	(i)
<u>PART I: Formation and Properties of Fibre-Reinforced Composites: Polyurethane Resins containing Polydiacetylene Single Crystal Fibres.</u>	
I.1 <u>Introduction</u>	1
I.2 <u>Experimental: Reactants and Reinforcements, Polymerisation Process and Materials Characterisation</u>	2
(a) Reactants	2
Niax triol LHT240	3
Trimethylol propane TMP	3
Polyisocyanate M340	3
(b) Reinforcing Fibres	3
Polydiacetylene fibres EUHD	3
Glass fibres HMG	3
(c) Polymerisation Process	3
(d) Materials Characterisation	4
Differential scanning calorimetry DSC	4
Dynamic mechanical-thermal analysis DMTA	4
Tensile properties	4
Charpy impact behaviour	4
Double torsion	5
I.3 <u>Results and Discussion</u>	5
(a) Tensile Stress-Strain Properties	5
(b) Charpy Impact Energy, G_{IC} , and Double Torsion Fracture Toughness, K_{IC} .	7
(c) Thermal Properties: DSC and DMTA	10
<u>PART II: Formation and Properties of Molecular Composites: Polyurethane-Diacetylene Segmented Copolymers.</u>	
II.1 <u>Introduction</u>	14
II.2 <u>Experimental</u>	15
(a) Synthesis, Purification and Characterisation of Reactants	15
4,4'-Methylenediphenylene diisocyanate MDI	16
Polyoxypropylene diols PPG1000 and PPG400	16
2,4-Hexadiyne-1,6 diol HDD	16
(b) Synthesis of Polyurethane Matrices and Polyurethane-diacetylene Copolymers	16
(c) Synthesis of Homopolyurethane Hard Segment HDD/MDI	18
(d) Materials Characterisation	19
II.3 <u>Results and Discussion</u>	19
(a) Thermal Properties: DSC	22
(b) Dynamic Mechanical-Thermal Behaviour	26
(c) Tensile Stress-Strain Properties	28

	Page
II.4 <u>Deformation Micromechanics of Urethane-Diacetylene</u>	29
<u>Copolymers using Raman Spectroscopy</u>	
(a) Raman Spectroscopy: Experimental	29
(b) Analysis and Discussion of Raman Spectra	30
<u>REFERENCES</u>	33

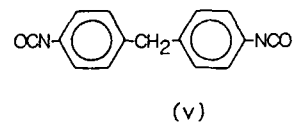
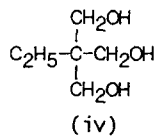
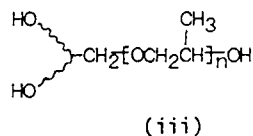
PART (I)Formation and Properties of Fibre-Reinforced Composites:
Polyurethane Resins containing Polydiacetylene Single Crystal FibresI.1 Introduction

For many engineering applications it is possible to increase the modulus and strength of thermosetting resins by incorporating reinforcing fibres. A reinforced resin consists of two main components: a matrix which may be thermosetting and a reinforcing filler which takes the form of fibres. In general the matrix has low strength in comparison to the reinforcement which is stiffer and often more brittle, and the combination of the two produces a material with intermediate stiffness and strength but whose toughness may be significantly superior due to the multitudinous interfaces present in the composite.

Numerous studies have been carried out on fibre-modified composites(5-8) and recently, much commercial interest has concentrated on fibre-reinforcement of brittle thermosetting resins, including in particular epoxy resins(9). Composites produced by incorporating high modulus fibres in a brittle matrix such as epoxy resin can have outstanding mechanical properties. Recent examples have included composites produced with high-modulus polyethylene fibres(10) and aromatic polyamide fibres (Kevlars)(11).

Polydiacetylene fibres offer great potential as reinforcement in brittle thermosetting matrices not only because of their superior stiffness and tensile strength, but also because of their low creep, good thermal stability and low density. Polydiacetylene single crystal fibres have recently been used as reinforcing agents in epoxy resins(12-14) and have been found to have promising mechanical properties.

Initial studies in this part of the research programme involved an investigation of the mechanical properties of polydiacetylene/polyurethane composites formed by incorporating pre-formed polydiacetylene fibres into a brittle thermosetting polyurethane matrix: these composites are analogous to those based on epoxy resins(13,14). Polyurethane composites have been moulded as plates containing different weight fractions (W_f) of randomly-oriented polydiacetylene fibres, formed by the solid-state polymerisation of the bis-(ethyl urethane) derivative of



Niax triol LHT240 (ex. Union Carbide) is a polyoxypropylene adduct of 1,2,6-hexanetriol and after drying by rotary film evaporation had an equivalent molar mass per OH group of 230 g mol^{-1} (by end-group acetylation).

Trimethylol propane TMP (ex. British Drug Houses) is a short chain triol of molar mass 134 g mol^{-1} and its melting point (by DSC) was determined as 56°C (lit. $56\text{--}57^\circ\text{C}$): TMP was therefore assumed to be pure and was used as-received.

Polyisocyanate M340 (ex. Dow Chemicals) is a liquefied form of MDI with a number average functionality of ~ 2.2 and an equivalent molar mass per NCO group of 161 g mol^{-1} determined by end-group analysis(19): M340 was used as-received.

(b) Reinforcing Fibres

Two different types of reinforcing fibres were used, namely, EUHD (polydiacetylene) fibres and HMG (glass) fibres.

Polydiacetylene fibres EUHD (ex. QMC Ind.Res.Ltd.) are faceted and deep-purple in colour with an average diameter of $30 \mu\text{m}$ and a mean fibre length of 5 mm .

Glass fibres (HMG) XG 1629 (ex. Turner Brothers) are $12 \mu\text{m}$ diameter and have a mean fibre length of $110 \mu\text{m}$: the fibres are not surface treated. The fibres were oven-dried ($120^\circ\text{C}/1\text{hr}$) before use.

(c) Polymerisation Process

All polymerisations (leading to the formation of both unfilled and filled materials) were carried out under essentially identical conditions using a single-step (one-shot), bulk process developed in previous studies(1). In all cases, the overall stoichiometric ratio, r , defined as the ratio of NCO to total OH groups, was kept constant at $r = 1.0$: reactions were carried out using an initial temperature of $50 \pm 1^\circ\text{C}$, without added catalysts.

The two polyol components, TMP and LHT240, were mixed in a 9:1 molar ratio under vacuum in a sealed flanged reaction vessel maintained at the required temperature (50°C). The liquid MDI, M340, pre-heated to 50°C was

then added to the polyol mixture, the vacuum re-applied and stirring resumed until all reactants were thoroughly mixed and the reaction mixture, initially cloudy, became clear. (When either iMG or EUHD fibres were incorporated they were completely dispersed in the polyol blend prior to the addition of the liquid MDI). Generally, after the addition of liquid MDI, the initially immiscible reactants became clear within four minutes and vitrification occurred after a further five minutes. All the polyurethane-forming reactions were exothermic even without added catalysts, and the temperature of the reaction mixture reached $\sim 155^{\circ}\text{C}$. In all cases the casting had to be completed within forty seconds from the time at which the mixture became clear.

(d) Materials Characterisation

Both unfilled and filled materials were characterised in terms of their thermal, dynamic-mechanical, tensile and fracture properties using the following techniques.

Differential Scanning Calorimetry, DSC, measurements were made on a Dupont 990 Thermal Analyser equipped with a DSC cell. Samples (~ 10 mg) and an inert reference material, glass beads (~ 10 mg) were encapsulated in aluminium pans and cooled to -120°C in the cell which was then heated in air at $20^{\circ}\text{C min}^{-1}$ to 250°C . Glass transition temperatures were determined from DSC traces as previously described(19): DSC traces were also used to assess the degradation behaviour of materials.

Dynamic Mechanical-Thermal Analysis, DMTA, was carried out on a Polymer Laboratories apparatus operating at a frequency of 1Hz in the temperature range -110 to 200°C at a heating rate of $5^{\circ}\text{C min}^{-1}$. A double-cantilever bending geometry was used for beam samples ($3 \times 10 \times 45$ mm) to obtain dynamic flexural moduli (E') and mechanical damping factors ($\tan\delta$) as functions of temperature.

Tensile Properties (ASTM D638M-81) were determined from the mean of at least 5 stress-strain experiments carried out at 23°C on an Instron 1122 Universal Testing Machine. Dumb-bell specimens were deformed to fracture at an extension rate of 5 mm min^{-1} , and tensile strains were determined accurately and independently of stress measurements using a 10% strain gauge extensometer.

Charpy Impact Behaviour was determined using a fully instrumented impact tester, designed and constructed at UMIST. Rectangular beam

specimens (3 x 10 x 50 mm) with span-to-depth ratios of 4 were tested in 3-point bending. Razor-sharp notches of varying length, a , were machined into the beams to give notch-to-depth ratios, a/D , in the range 0.1 to 0.5 (see fig 1(a)). About 60 specimens for each material were impact tested at 23°C using an initial impact velocity of 4.5 m s^{-1} .

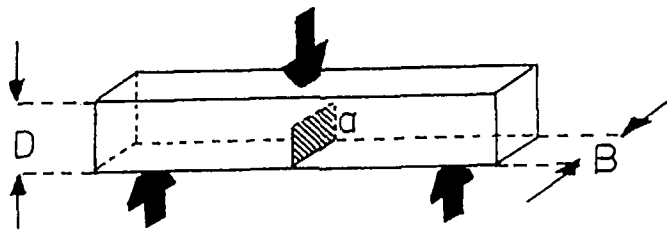
Double Torsion tests were used to evaluate the fracture toughness, under slow crack-growth conditions, for each material. Rectangular plate specimens (3 x 35 x 100 mm), each containing a V-shaped centre groove (~1 mm deep) along the bottom face, were used in double torsion tests. A sloping notch was introduced at one end of the specimen, and sharpened using a razor blade. Grooved plates were deformed at 23°C on an Instron 1122 in the compression mode, using the special rig shown in fig. 1(b). The specimen, supported on the two parallel rollers with the centre-groove on the bottom face, is loaded using the two hemispheres at the notched end. The testing rate used was 2 mm min^{-1} .

I.3 Results and Discussion

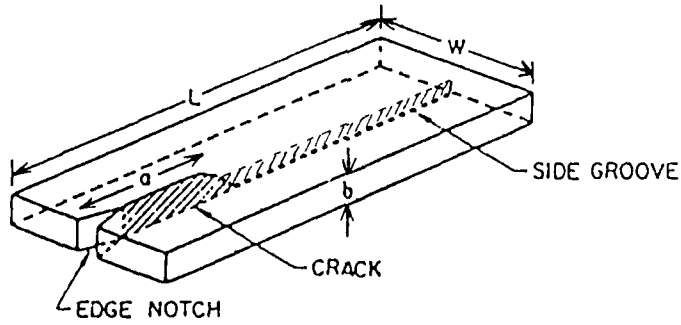
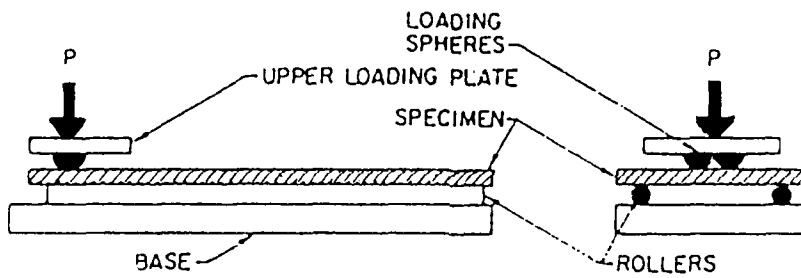
The unfilled polyurethane (PU) resin is a highly-crosslinked polymer which at room temperature is a glassy, amorphous material with properties(1) similar to the epoxy resins commonly used as matrices for composites. The degree of reinforcement of the PU resin, attained by incorporating fibres, depends principally on (a) fibre content (expressed as a weight fraction, W_f), (b) fibre aspect ratio (length-to-diameter, l/d) and (c) fibre-matrix interfacial bonding. In these studies, the amount of EUHD fibres that could be incorporated into PU formulations was severely limited to $W_f \ll 0.05$, due to extremely high viscosities produced during the processing of composite materials, which made casting virtually impossible. In contrast, the lower aspect ratio and higher bulk density of the HMG fibres meant that higher fibre contents, $W_f \ll 0.30$, were readily achievable. Given these limitations, two comparative series of PU composites namely, PU-EUHD with $0 \ll W_f \ll 0.5$ and PU-HMG with $0 \ll W_f \ll 0.30$, were produced and characterised using the process and experimental techniques described.

(a) Tensile Stress-Strain Properties

Average stress-strain curves are shown in fig 2 and 3 for the PU-EUHD and PU-HMG series, respectively. Tensile properties in terms of Young's modulus (E), tensile strength (σ_U), ultimate elongation (ϵ_U) and tensile toughness (U_t , the total area under a stress-strain curve) have been derived



(a)



(b)

Figure 1. Fracture specimen geometries used to determine (a) G_{IC} from three-point bend, Charpy impact tests; (b) K_{IC} from double-torsion tests.

from each curve in fig 2 and 3, and are summarised in Table 1.

The unfilled matrix, PU-0, shows essentially brittle behaviour under slow tensile deformation with slight evidence of yielding around 8% strain followed almost immediately by brittle fracture at about 10% strain. Incorporating fibres, even at W_f as low as 1% in the case of EUHD, totally

Table 1. Tensile Properties of Unfilled PU and PU-EUHD and PU-HMG Composites

Material	W_f (%)	E (GPa)	σ_u (MPa)	ϵ_u (%)	U_t (MJ m ⁻³)
PU-0	0	3.25	88.7	9.6	6.2
PU-EUHD-1	1	3.60	84.2	4.5	2.4
PU-EUHD-2	2	3.95	84.8	3.9	1.9
PU-EUHD-3	3	4.25	86.5	3.4	1.7
PU-EUHD-4	4	4.52	90.4	3.2	1.6
PU-EUHD-5	5	4.70	89.7	2.8	1.4
PU-HMG-10	10	4.13	91.5	5.0	2.7
PU-HMG-20	20	4.83	95.2	3.5	2.2
PU-HMG-30	30	5.92	95.4	2.5	1.9

suppresses any possibility of yielding and transforms PU-0 into a completely brittle material. For both series of composites, modulus is seen to increase with W_f but at a higher rate for the PU-EUHD composites as shown in the top plot of fig 4. Tensile strength of the PU-EUHD composites shows a sudden, initial decrease to a minimum value at 1% W_f , (middle plot, fig 4) and then rises to a value which at 5% W_f , just exceeds that of the unfilled matrix. In contrast, tensile strength of PU-HMG composites shows a progressive increase with W_f , with σ_u reaching an apparently limiting value at W_f between 20 and 30%. Ultimate elongation shows the expected decrease with increasing W_f for both series (bottom plot, fig 4), with ϵ_u for the PU-EUHD composites decreasing much more rapidly over the initial 5%

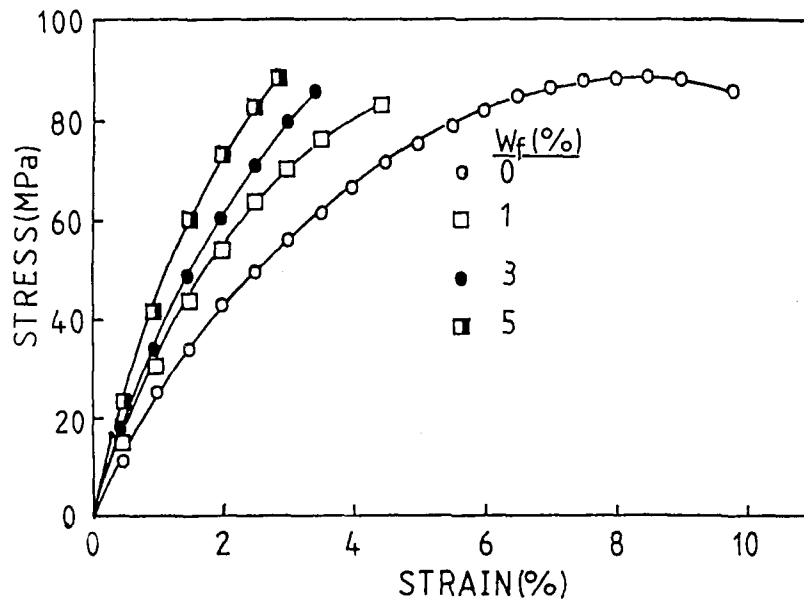


Figure 2. Average tensile stress-strain curves for unfilled PU and PU-EUHD composites.

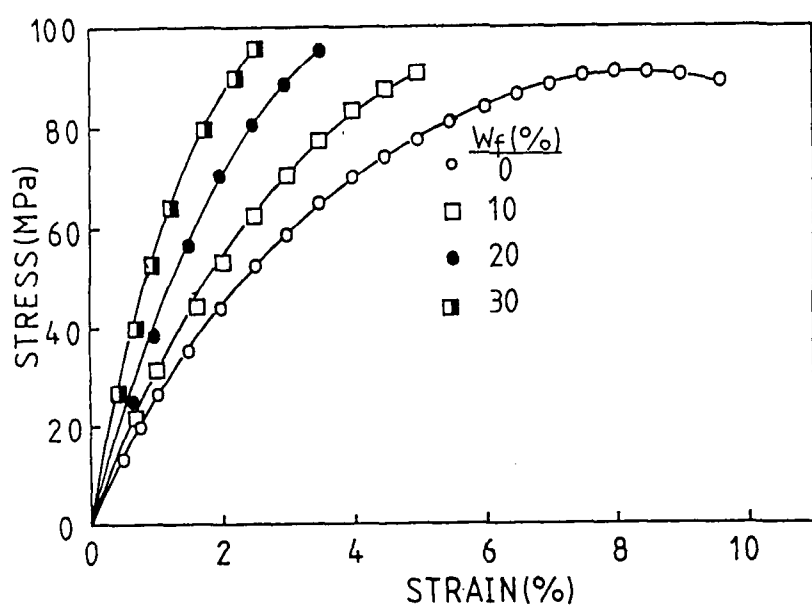


Figure 3. Average tensile stress-strain curves for unfilled PU and PU-HMG composites.

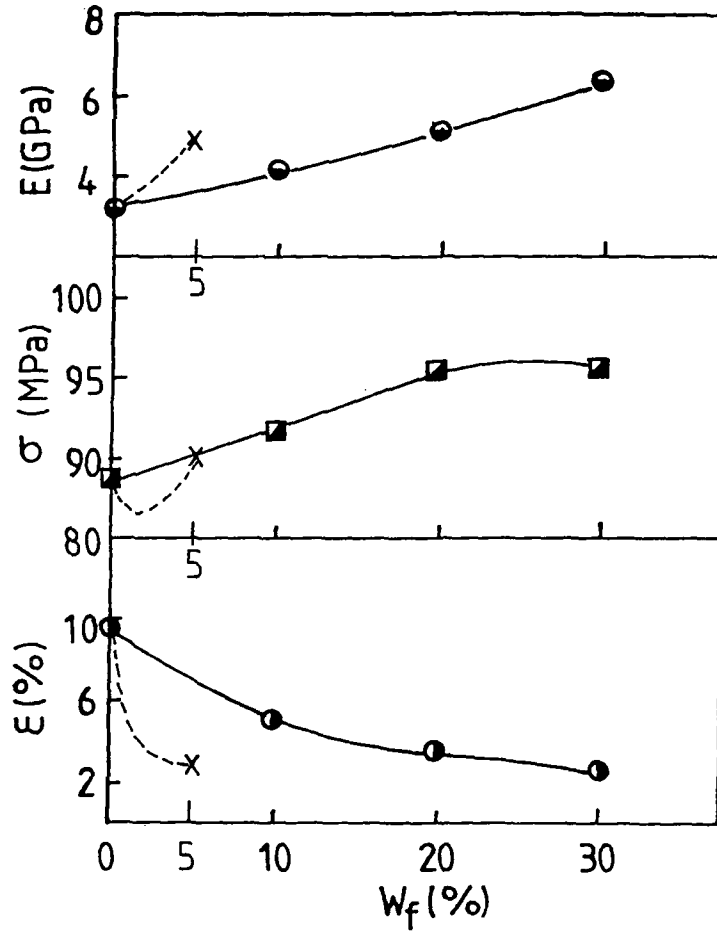


Figure 4. Variation of tensile modulus (E), strength (σ) and ultimate elongation (ϵ) with fibre content (W_f) for PU-HMG composites. Dashed lines show corresponding trends for PU-EUHD composites up to the maximum achievable W_f of 5% shown by the single datum points, -X-.

W_f region. These trends in composite properties, given the similarity between the tensile properties of EUHD and HMG fibres, depend mainly on fibre aspect ratio and fibre-matrix, interfacial bond strength. Thus inspite of the higher aspect ratio of EUHD fibres, which is responsible for the higher composite stiffness (at low strains), the poor level of interfacial bonding in PU-EUHD composites probably accounts for the greater deleterious effects (at high strains) on tensile strength and ultimate elongation, and hence on material toughness, as W_f increases.

(b) Charpy Impact Energy G_{IC} , and Double Torsion Fracture Toughness, K_{IC}

The use of an instrumented impact apparatus enables continuous force-time data to be recorded and stored over the complete impact event, typically ~1 ms. Thus, as illustrated in fig 5, the characteristic shape of the impact curve, the maximum or peak force and displacement and the fracture energy (proportional to the shaded area) can be determined for each particular material. Charpy impact data for the various EUHD- and HMG- polyurethane composites were analysed using a linear elastic fracture mechanics (LEFM) analysis(20), which relates the fracture energy, W , to propagate a crack of initial length, a , to the reduced cross-sectional area, $BD\phi$ of a beam, according to eqn (1) and (2):

$$W = G_{IC}.BD\phi \quad (1)$$

$$\phi = \frac{\int Y^2(a/D).da + S/18}{Y^2a} \quad (2)$$

In eqn (1), G_{IC} is the critical strain energy release rate and ϕ is a geometrical factor which, for a given span-to-depth ratio, S/D , accounts for variations in notch-to-depth ratio, a/D , through the fourth degree polynomial term, Y , in eqn (2). For each material, the experimental impact data, obtained from force-deflection curves similar to those shown in fig 5, showed very good correlation with LEFM, and plots of W versus $BD\phi$ were essentially linear and extrapolated to the origin, $W = BD\phi = 0$. The values of G_{IC} for all materials were determined from the slopes of W versus $BD\phi$ plots, using least-squares analysis, and are listed in the second column of Table 2.

Double torsion tests, compared with Charpy impact tests, are relatively slow crack-growth measurements which lead directly to the evaluation of

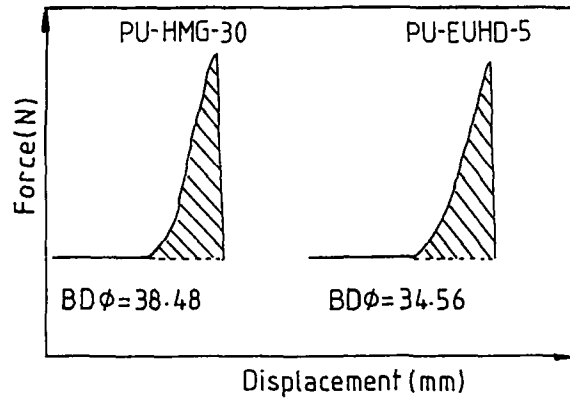


Figure 5. Typical force-displacement curves obtained from Charpy impact specimens of PU-HMG-30 and PU-EUHD-5 composites of similar dimensions, $BD\phi$.

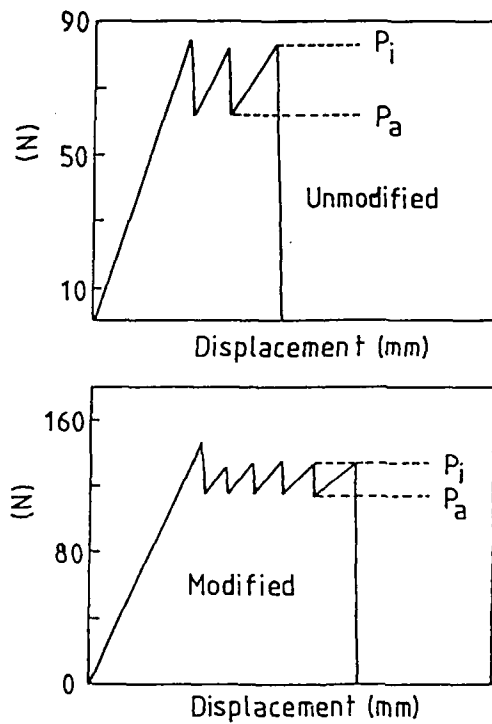


Figure 6. Typical force-displacement curves obtained from double torsion specimens of unfilled PU and fibre-modified PU. Curves show unstable-brittle crack propagation behaviour with P_i and P_a the forces at crack initiation and arrest, respectively.

fracture toughness, K_{IC} , according to eqn (3),

$$K_{IC} = P_C L_m \left[\frac{1 + \nu}{L_W b^3 b_n k} \right]^{1/2} \quad (3)$$

where P_C is the critical load, L_m the moment arm, ν the Poisson's ratio of the material, W and B are the width and thickness of the plate, and t_n is the plate thickness above the groove. The dimensionless parameter, k , is a function of the ratio $W/2b$ and allows for errors in evaluating K_{IC} for specimens of finite width(21). In general, three types of load-displacement curve have been identified(22) which correspond to different modes of crack propagation during double torsion tests. These are (a) stable-brittle propagation, (b) unstable-brittle propagation and (c) stable-ductile propagation. All of the polyurethane materials (unfilled and filled) investigated in this study failed by unstable-brittle crack propagation which exhibits the characteristic intermittent stick-slip, load-displacement behaviour as shown by the curves in fig 6. The values of P_i and P_a correspond to the loads at crack initiation and arrest, respectively, from which stress intensity factors (fracture toughness), K_{ICi} and K_{ICa} , can be determined using eqn(3). These values for each material are listed in the third and fourth columns of Table 2.

There are distinct differences in fracture behaviour between the EUHD- and HMG-composites in terms of the trends of G_{IC} and K_{IC} with fibre content. These differences are more clearly illustrated by plotting the data in Table 2 in the form of G_{IC} versus W_f as in fig 7, and K_{IC} (initiation and arrest) as in fig 8. In the case of fracture energy for crack propagation under impact loading, G_{IC} for PU-EUHD composites shows a small initial decrease and then rises very sharply over the small W_f range (1 to 5%), whereas for the PU-HMG composites, there is a more significant initial decrease before rising more gradually to a final value at 30% W_f which only just exceeds G_{IC} (1.86 kJ m⁻²) for the unfilled PU resin. These observations appear to confirm those discussed in the previous section on tensile properties, in that the higher aspect ratio and more poorly bonded EUHD fibres, compared with HMG fibres, give rise to greater energy absorption by debonding and pull-out failure mechanisms during overall fracture. That the trend in G_{IC} with W_f is opposite to that of U_t (tensile

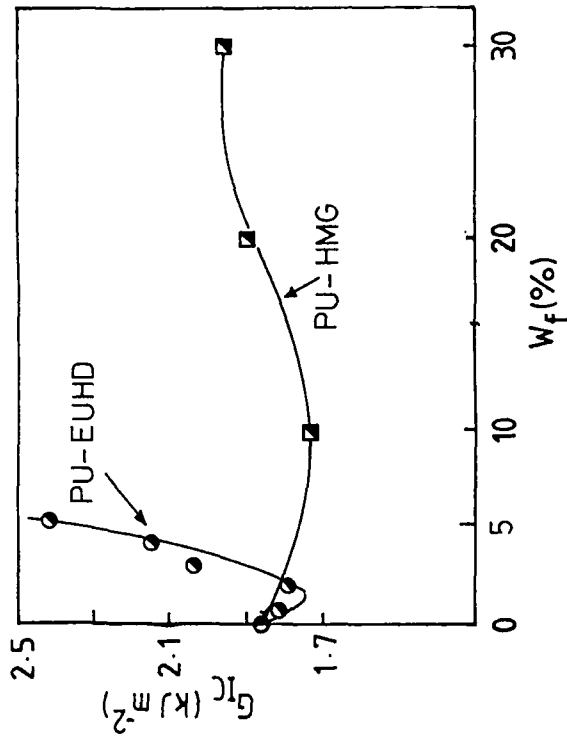


Figure 7 (above). Variation of G_{IC} (determined from Charpy impact measurements) with fibre content, W_f , for PU-EUHD and PU-HMG composites.

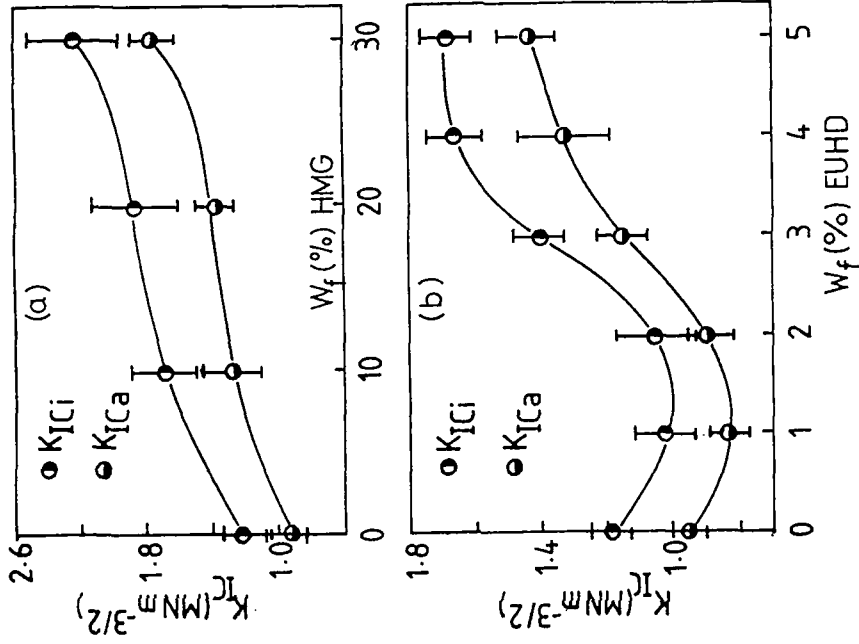


Figure 8 (right). Variation of K_{IC} (determined from double torsion measurements) with fibre content, W_f , for (a) PU-EUHD composites and (b) PU-HMG composites. Subscripts i and a refer to initiation and arrest data.

toughness) is attributed to the quite different tests and the basis on which these fracture parameters are determined. G_{IC} is a measure of the

Table 2. Fracture Properties of Unfilled PU Resin, PU-EUHD and PU-HMG Composites

Material	W_f (%)	G_{IC} (kJ m ⁻²)	K_{ICi} (MN m ^{-3/2})	K_{ICa} (MN m ^{-3/2})
PU-O	0	1.86	1.19	0.95
PU-EUHD-1	1	1.85	1.02	0.82
PU-EUHD-2	2	1.80	1.05	0.89
PU-EUHD-3	3	2.05	1.40	1.14
PU-EUHD-4	4	2.14	1.67	1.33
PU-EUHD-5	5	2.39	1.68	1.43
PU-HMG-10	10	1.73	1.68	1.29
PU-HMG-20	20	1.89	1.86	1.37
PU-HMG-30	30	1.95	2.22	1.78

energy required to propagate a sharp, pre-existing crack under high-speed impact conditions. In contrast, U_t , which decreases sharply with W_f almost identically to ϵ_u as shown in the bottom plot of fig 4, measures the total energy (initiation and propagation) of fracture for an un-notched material subjected to much slower deformation rates.

Considering fracture toughness (K_{IC}), the same arguments may again be applied to account for the different trends with W_f compared with those for U_t . That is, K_{IC} is a measure of the stress intensity causing fracture initiation at the tip of a sharp, pre-existing crack (even though the deformation rates used in tensile and double torsion tests are similar). Comparing the fracture toughness of PU-EUHD and PU-HMG composites, fig 8 shows that at low W_f , K_{IC} for the former decreases initially whereas K_{IC} for the latter appears to increase steadily. The poor fibre-matrix bonding in PU-EUHD composites means that only low localised stresses are required to cause debonding at fibre ends, leading to extensive matrix micro-cavitation which then provides additional stress concentration and

initiates overall failure at lower loads, P_C (see eqn (3)). Despite the poor bonding, at higher W_f (>2%) however, some load transfer to EUHD-fibres must be occurring at slow deformation rates since, as seen in Table 1, σ_U for PU-EUHD composites does eventually show a slight increase over that for the unfilled PU. As K_{IC} is determined by P_C , the overall peak load causing crack initiation, then K_{IC} should follow the same trend as σ_U with W_f , as is the case. The reversal in K_{IC} (fig 8), however, is difficult to interpret but does imply a change in failure mechanism at higher W_f . In contrast to the PU-EUHD composites, those containing better bonded HMG fibres show a progressive rise in fracture toughness as W_f increases (fig 8), reaching a value of K_{IC} almost twice that of the unfilled PU resin (1.19 (initiation) and 0.95 (arrest) $MN m^{-3/2}$). To summarise, the highly notch-sensitive (unfilled) PU resin is transformed into a relatively notch-insensitive material by incorporating modest levels of discontinuous fibres. The use of polydiacetylene fibres, although restricted to low W_f , does result in composite materials with superior stiffness and impact resistance compared with glass fibres, although the latter give rise to composites with higher tensile strengths and fracture toughness.

(c) Thermal Properties: Differential Scanning Calorimetry and Dynamic Mechanical Analysis

The thermal characterisation of composite materials is extremely important both at the practical level, in terms of dimensional stability and resistance to degradation during high-temperature applications, and at the fundamental level in terms of transitional and relaxational behaviour which enables interpretation of the complex interactions between fibres and matrix. Such information is obtained from DSC and DMTA data.

Typical DSC curves are shown in fig 9 for three materials, the unfilled matrix, PU-0, and composites PU-HMG-30 and PU-EUHD-5. Only two thermal events were observed for all materials over the temperature range studied (-120 to 250°C). The transition occurring between 150 and 160°C is the glass transition temperature, T_g , of the material, the value of which is obtained from the intersection of the tangents drawn to the base line and the endothermic change in slope. The other thermal event is shown as the exothermic upturn in DSC traces which is associated with thermal degradation, and a temperature, T_d , defined as the onset temperature for degradation, can be determined from the deviation of the DSC curve from the

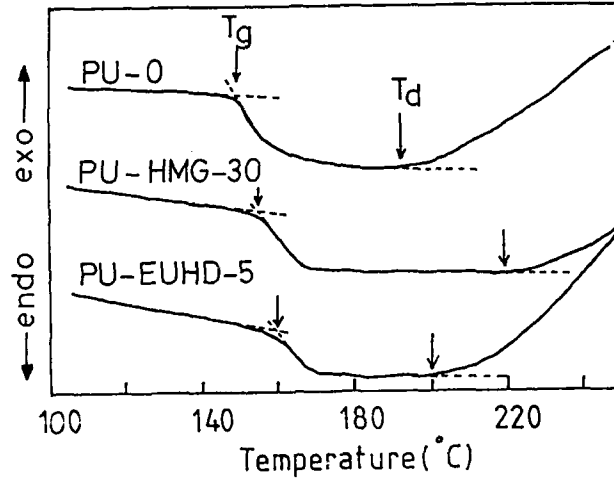


Figure 9. Typical DSC curves for unfilled PU, and PU-HMG and PU-EUHD composites, showing the locations of glass transitions, T_g , and onset degradation, T_d .

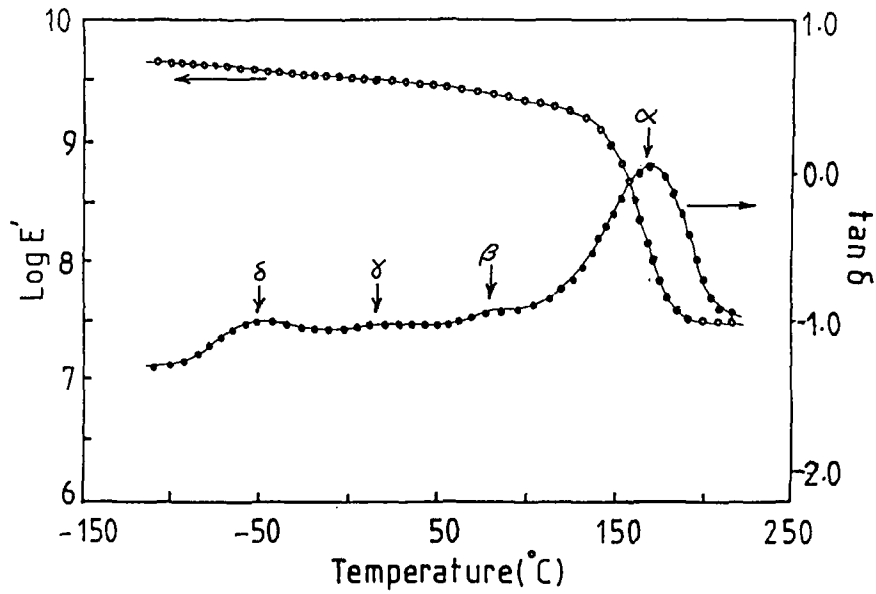


Figure 10. DMTA curves for PU-EUHD-1 showing storage flexural modulus (E') and mechanical damping ($\tan \delta$) versus temperature. The major peak (α) corresponds to the glass transition: secondary relaxations are designated β , γ and δ .

extrapolated portion of the baseline above T_g . Values of T_g and T_d , which are the mean of several determinations ($\pm 1^\circ\text{C}$), are listed in the third and fourth columns of Table 3.

The T_g values (DSC) in Table 3 show a progressive increase as W_f increases for both types of composite. An increase in T_g indicates reduced segmental mobility in the PU matrix arising from interactions with fibre surfaces. In the case of HMG, reaction between silanol groups on the surface of glass with $-\text{NCO}$ groups in the PU-forming system during composite preparation leads to covalent bonding (surface coupling) and consequently to strong and permanent fibre-matrix bonding. However, the increase in T_g for PU-HMG composites is only modest even with 30% W_f . In contrast, the increase in T_g for PU-EUHD composites is significantly greater over a much smaller W_f range. This must be due to the development of weaker but more extensive interactions resulting from hydrogen-bonding between urethane groups, in substituents attached to polydiacetylene chains in EUHD fibres, and the urethane and ether groups in the PU matrix.

Table 3. Thermal Properties of Unfilled PU, PU-EUHD and PU-HMG Composites

Material	W_f (%)	DSC		DMTA	
		T_g ($^\circ\text{C}$)	T_d ($^\circ\text{C}$)	α or T_g ($^\circ\text{C}$)	δ ($^\circ\text{C}$)
PU-0	0	151	195	163	-60
PU-EUHD-1	1	151	200	163	-52
PU-EUHD-2	2	152	200	163	-52
PU-EUHD-3	3	155	200	168	-52
PU-EUHD-4	4	165	200	170	-49
PU-EUHD-5	5	167	200	172	-50
PU-HMG-10	10	153	220	167	-60
PU-HMG-20	20	155	220	169	-60
PU-HMG-30	30	158	220	171	-60

Resistance to thermal degradation of the unfilled matrix is determined mainly by the stability of the ether groups of the LHT240 component forming PU-O. Incorporating essentially inert glass fibres delays the onset of degradation as seen by the increase in T_d from 195 to 220°C and also reduces the rate of degradation as indicated by the lower slope of the exothermic curve in fig 9. In contrast, only a slight increase in T_d (5°C) is observed for EUHD-fibre composites compared with PU-O, but much more significantly the rate of degradation is much greater as shown by the bottom curve of fig 9. Indeed, in a separate series of experiments using thermal gravimetry (TG) at 200°C in air on isolated EUHD fibres, weight losses of up to 60% were recorded which were attributed to the thermal instability of ethyl urethane groups in EUHD: the weight loss of HMG was negligible under the same conditions.

Dynamic mechanical-thermal analysis provides modulus-temperature and molecular relaxation behaviour of composite materials. Typical plots of $\log(E')$ and $\tan \delta$ versus temperature are shown in fig 10 for PU-EUHD-1. Incorporating fibres increases the level of modulus-temperature curves and the large decrease in $\log(E')$ over the glass transition region (almost 3 decades for unfilled PU-O) is progressively reduced in both series of composites as fibre content (W_f) increases. Similarly, mechanical damping, $\tan \delta$, (including peak intensities) is reduced as W_f increases. The damping curves ($\tan \delta$ versus temperature plots) for all materials showed the four relaxations indicated in fig 10 which, in order of decreasing temperature are designated α , β , γ and δ . The α -peak, clearly the most intense, is associated with the glass transition, and the lower, less-intense peaks and shoulders are secondary relaxations associated with more specific molecular motions occurring within the matrix. The β -relaxation between 50 and 100°C is probably due to dissociation of hydrogen-bonding in urethane (including ether) groups; the γ -relaxation between -20 and 40°C may be due to dissociation of either "free" water (incorporated by moisture absorption) or "bound" water if it has associated with urethane groups. The lowest temperature, δ -relaxation between -60 and -50°C, arises from segmental motion of oxypropylene units in the LHT240 component (isolated $T_g \approx -60^\circ\text{C}$) of the matrix.

Values of the α - and β -relaxation temperatures are listed in the final two columns of Table 3. The α -relaxation (or T_g) is dominated by the high

aromatic content (66% by weight) in the PU matrix. Again, for both series of composites, there are progressive increases in T_g with increasing W_f and the explanation for these trends is the same as for the DSC data. The other point of interest concerns the location of the δ -relaxation which, as Table 3 shows, is unaffected (at -60°C) by the incorporation of upto 30% W_f of HMG, whereas there is an upward shift of about 10°C to $\sim -50^\circ\text{C}$ with much smaller amounts of EUHD fibres. The δ -peak is associated with molecular relaxations of the polyether chains ($\sim 12\%$ by weight) in the PU matrix. The polyether and aromatic components of the PU matrix are intrinsically incompatible and will phase-separate on the molecular level (despite the apparent optical clarity of PU-O in visible light). As discussed, there is a high potential for hydrogen-bonding between the ethyl urethane groups on EUHD fibres and the ether oxygens in the LHT240 component of the matrix. This hydrogen-bonding will tend to compatibilise the polyether and aromatic phases, and promote phase-mixing. Adsorption of polyether segments onto relatively stiff EUHD fibres also occurs and reduces segmental motion in the former. Consequently, there will be an upward shift in the temperature location of the δ -relaxation.

In summary, thermal characterisation, particularly in terms of shifts in T_g , indicates varying degrees of fibre-matrix interactions in both series of composites: covalent bonding in HMG-composites and extensive hydrogen-bonding in EUHD-composites. These observations would appear to be contradictory to those reported in the tensile and fracture section which showed the EUHD fibres to be more poorly bonded than HMG fibres. This contradiction is probably explained in terms of the relative strengths of covalent and hydrogen-bonding interactions, with the latter showing less resistance to even low levels of deformation.

PART (II)Formation and Properties of Molecular Composites:Polyurethane-Diacetylene Segmented CopolymersII.1 Introduction

Segmented copolyurethanes are characterised by a two-phase morphological structure comprising incompatible rigid, glassy hard segments (HS) and extensible, rubbery soft segments (SS). The detailed morphology depends primarily on the relative proportions of HS and SS: at low HS contents, the rubbery SS form the continuous phase in which dispersed HS domains act essentially as a reinforcing filler and multifunctional crosslinks(23). At high HS contents, phase inversion can occur and the copolyurethane may be regarded as a rubber-toughened plastic in which the HS form the continuous phase and the SS are dispersed rubber particles. Seldom is phase separation complete, particularly in copolyurethanes in which appreciable hydrogen bonding between HS and SS occurs(24). Consequently, the transition from one morphology to the other is not sharp and at intermediate HS contents, the copolymer may comprise a bi-continuous and interpenetrating, two-phase structure.

The nature of the morphological structure largely determines the properties of segmented copolyurethanes. The mechanical properties in particular depend not only on HS content but also on HS domain size, the cohesive strength of the domains and their ability to orient in the direction of an applied deformation: the deformation behaviour of the SS phase also affects copolymer properties, but to a lesser extent(24). Clearly, for a segmented copolyurethane subjected to deformation, the distributions of stress and strain between HS and SS phases will be different. Attempts(25,26) have been made using IR dichroism to investigate the response of HS in copolyurethanes subjected to low and high strains, but the results yielded only information concerning HS orientation. A more specific analytical technique is therefore necessary to study the detailed deformation behaviour within an individual phase. It then follows that the chemical and topological structure of the phase must be well-defined and quantitatively responsive to the technique employed.

Previous studies(27-29) have shown that phase-separated copolymers containing highly spectroscopically-active HS phases based on

cross-polymerised poly(diacetylene)s, can be formed under controlled synthesis conditions. In particular, copolyurethanes comprising SS based on a polyoxytetramethylene diol ($M_n = 1,000 \text{ g mol}^{-1}$) and HS formed from either hexamethylene diisocyanate (HDI) or 4,4'-methylenediphenylene diisocyanate (MDI) reacted with either 2,4-hexadiyne-1,6 diol (HDD) or 5,7-dodecadiyne-1,12 diol (DDD), were shown after controlled cross-polymerisation to be active to Raman spectroscopy(29). HS contents were in the range 19 to 24% w/w and cross-polymerisation to varying degrees was effected by thermal and γ -radiation treatments. The use of Raman spectroscopy was limited to characterising only undeformed copolyurethanes to demonstrate the presence of conjugated poly(diacetylene) moieties within HS phases, in relation to the detailed chemical structure of the HS repeat units.

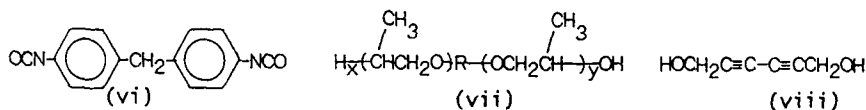
Raman spectroscopy, however, has been used much more effectively to yield quantitative information on the deformation of substituted poly(diacetylene), single-crystal fibres(30-32).

Part II of this report presents results of studies on the structure-property relations in segmented copolyurethanes comprising completely amorphous SS, based on polyoxypropylene (PPG) diols, and thermally cross-polymerised poly(diacetylene) HS formed from MDI and HDD. Specifically, the distributions of localised stress and strain within HS phases have been studied by Raman spectroscopy applied to the copolyurethanes subjected to simultaneous tensile deformation.

II.2 Experimental

(a) Synthesis, Purification and Characterisation of Reactants

Two linear polyurethanes, with T_g values of -28 and 26°C (by DSC), were used as the continuous, soft segment matrix materials in the molecular composites. The PU's were formed from reactants whose chemical structures are shown below, namely, pure MDI (vi) and each of two polyoxypropylene diols (vii), PPG1000 and PPG400, for which $(x + y) = 6$ and 16 , respectively. In the segmented copolyurethanes, the discontinuous, reinforcing phase comprised rigid hard segments formed from MDI and the low molar mass, diol chain extender (viii), 2,4-hexadiyne-1,6 diol, HDD.



4,4'-Methylenediphenylene Diisocyanate, MDI, (ex. BDH). The aromatic MDI, in flake form, was melted and filtered through a grade 4 sinter (50°C) using a Buchner flask and water pump (10mm Hg). The equivalent weight of the MDI was determined by -NCO titration to be 125 g mol⁻¹.

Polyoxypropylene Diols, PPG400 and PPG1000, (ex. BDH). Both diol pre-polymers were dried by vacuum rotary film evaporation (100°C/0.3 mm Hg) for 5 hours. Characterisation was carried out using end-group acetylation(34) to give equivalent weights (that is, molar masses per functional group) of 203 and 498 g mol⁻¹, respectively, for PPG400 and PPG1000.

2,4-Hexadiyne-1,6 Diol, HDD. This reactant was synthesised from propargyl alcohol (ex. Fluka Chemicals) according to the procedure reported by Hay(35), and was re-crystallised from boiling toluene (111°C) and vacuum dried (90°C/4h) prior to use. The pure HDD was obtained as fine white crystals and had a melting point of 112°C (lit. 109-113°C).

(b) Synthesis of Polyurethane Matrices and Polyurethane-Diacetylene

Copolymers

The two linear polyurethanes (isolated soft-segment homopolymers formed from MDI and each PPG) and the corresponding polyurethane-diacetylene copolymers were all formed in bulk, using a one-step polymerisation process to simulate industrial processes such as reaction injection moulding, RIM.

The rapid development of RIM has resulted in significant increases in the productions of polyurethane materials, particularly segmented copolyurethane elastomers. The formation of such elastomers by RIM is by definition a one-step, bulk copolymerisation process(2) in which one reactant stream comprises a blend of polyether pre-polymer and diol chain extender and the other reactant stream is a liquefied form of MDI. In this context, the polyurethane-diacetylene segmented copolymers studied in the present work were formed by a hand-casting technique involving a similar one-step, bulk (rather than solution) copolymerisation process which therefore overcomes the subsequent need to remove solvent. This process is in distinct contrast to the multi-step, solution method employed by other workers(27-29) and provides an interesting comparison in terms of the structures and properties of the copolymers produced. In the bulk process, a significant rise in temperature due to the polymerisation exotherm is inevitable and some cross-polymerisation of the diacetylene-based HS will always occur, which is not the case in the solution process. In addition,

the one-step process enables HS of greater length to form although the distribution of HS lengths is broader than in the multi-step process. Consequently, in the phase-separated copolyurethane, the HS domains are less well-defined and are more easily disrupted when subjected to temperature and deformation.

In the present studies, urethane homopolymers and copolymers were formed using a single-step or one-shot process(1). In all cases, polymerisations were carried out without catalysts using an overall stoichiometric ratio, r , of unity and an initial reaction temperature of $80 \pm 1^\circ\text{C}$. Formulations, based on the different proportions by weight of reactants used to form the various polymers, are given in Table 4.

Table. 4. Relative Parts by Weight of Reactants used to Form Various Homopolyurethanes and Polyurethane-Diacetylene Copolymers

Material Reactant	PPG1000/MDI	PPG1000/HDD/MDI	PPG400/MDI	PPG400/HDD/MDI	HDD/MDI
MDI	1.00	1.00	1.00	1.00	1.00
HDD	-	0.22	-	0.22	0.44
PPG1000	3.87	1.99	-	-	-
PPG400	-	-	1.60	0.81	-

Typically, between 50 and 100 g of total reactants were used in formulations. In the segmented copolyurethanes, the molar ratios of reactants were $\text{PPG:HDD:MDI} \approx 1:1:2$ and the weight percentages of diacetylene-based hard segments in PPG1000/HDD/MDI and PPG400/HDD/MDI were 22.4 and 35.5, respectively. Hard segment content is defined as the mass of HDD plus the stoichiometric equivalent of MDI divided by the total mass of the formulation. In a typical preparation, the PPG diol and the stoichiometric equivalent amount of HDD were weighed accurately into a 250ml sealed flanged reaction vessel, equipped with a stirrer, and immersed

in a thermostated water bath ($80 \pm 1^\circ$). The pale yellow reaction mixture was stirred and de-gassed by applying vacuum (~ 0.3 mm Hg). (In the case of homopolyurethanes, HDD was omitted.) The stoichiometric equivalent amount of molten MDI was then added to the polyol blend via a heated glass funnel. The complete reaction mixture was stirred continuously for 2 hours at 80°C (although the initial reaction exotherm raised the temperature to $\sim 120^\circ\text{C}$ for a few minutes). During the reaction time, the initial clear mixture became cloudy as the polymerising diacetylene-urethane hard segments and polyether-urethane soft segments phase-separated: there was also a colour change from pale yellow to deep orange-brown and an increase in viscosity as the overall molar mass increased. After the 2 hour period, vacuum was re-applied to de-gas the reaction mixture which was cast into picture-frame moulds, previously sprayed with silicone release agent and pre-heated to 80°C . (Some of the reaction mixture, which became semi-solid at room temperature, was kept for subsequent thermal analysis by DSC). Polymerisation of the reaction mixtures was then completed by subjecting the cast materials to a curing schedule of 120°C for 36 hours. There was a further colour change during curing to deep purple and DSC experiments, described later, showed that no further reaction could be achieved. The cured copolyurethanes were stored in a vacuum desiccator containing silica-gel until subsequent testing. (The homopolyurethane soft-segment materials, PPG1000/MDI (an elastomer) and PPG400/MDI (a soft, ductile plastic), were transparent, pale yellow materials: that is, no colour changes occurred during preparation and curing).

(c) Synthesis of Homopolyurethane Hard Segment, HDD/MDI

In contrast to the homopolyurethane soft segments, PPG1000/MDI and PPG400/MDI, and the corresponding diacetylene-urethane copolymers, which were all formed in bulk, the homopolyurethane hard segment material, HDD/MDI, could only be formed in solution. As shown in the last column of Table 4, HDD/MDI was synthesised from stoichiometric equivalent amounts of pure HDD and MDI in freshly-distilled dimethylformamide (DMF) solution. The HDD (~ 15 g) was weighted accurately into a 50 ml flanged reaction vessel to which DMF

(7.5 ml) was added to dissolve fully the HDD at 21°C . The sealed reaction vessel was fitted with a mechanical stirrer and then immersed in a glass-sided, thermostated water bath at $40 \pm 1^\circ\text{C}$. The HDD solution was stirred and de-gassed simultaneously (~ 0.3 mm Hg) by means of a rotary

vacuum pump. The required amount (~35 g) of MDI was accurately weighted and added to the HDD solution via a warmed glass funnel, and the total reaction mixture was stirred and de-gassed for 2 minutes. Initially, the HDD/MDI/DMF reaction mixture was a clear, pale yellow colour and during the 2 minutes period the reaction mixture became progressively cloudier as phase separation between polymer and DMF solvent occurred. After 2 minutes, the reaction exotherm had increased the temperature to ~150°C and the cloudy reaction mixture became orange-brown in colour. The partially-polymerised mixture was poured into a pre-heated (80°C) picture-frame mould which was placed in an oven for 6 hours at 120°C at atmospheric pressure and then in a vacuum oven at 120°C for a further 30 hours to effect complete reaction and to remove all the DMF. After the first 6 hours at 120°C, the colour of the sample had turned dark brown, and after complete reaction (36 hours) the HS homopolyurethane was a deep brown-purple colour.

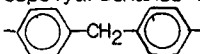
(d) Materials Characterisation

Homopolyurethanes and urethane-diacetylene copolymers were characterised in terms of the thermal, dynamic-mechanical and tensile properties using the techniques described in Part I (section I.2(d)) of this report. In addition, a detailed investigation of the micromechanics of deformation of the copolyurethanes was carried out using a specially-modified Raman spectroscopy technique. Details of this technique and of the analysis of derived data are given in a later section.

II.3 Results and Discussion

The homopolyurethane soft segments, PPG1000/MDI and PPG400/MDI are linear amorphous materials which at room temperature are, respectively, a soft elastomer and a "leathery", ductile plastic. The homopolyurethane hard segment, HDD/MDI, after cross-polymerisation (see later), is a highly-crosslinked material which at room temperature is a glassy but ductile plastic. In the urethane-diacetylene copolymers, which may be described as molecular composites, the degree of reinforcement of the soft segment attained by incorporating dispersed hard segments, depends on (a) hard segment content (expressed as a weight percentage, HS%), (b) the degree of phase separation and connectivity between hard and soft segments, and (c) the degree of crosslinking in the hard segment, achieved by thermal cross-polymerisation of the diacetylene moieties.

The poly(urethane-diacetylene) materials are more accurately described

as segmented block copolymers of the $-(AB)_n$ type in which the hard (A) and soft (B) segment blocks phase separate to yield a bulk material comprising a soft polyether matrix reinforced with hard glassy domains. A simplified reaction scheme showing the formation of the segmented block copolyurethanes from reactants (vi) to (viii) in which $-R-$ is , is shown in fig. 11. Ideally, block copolymers

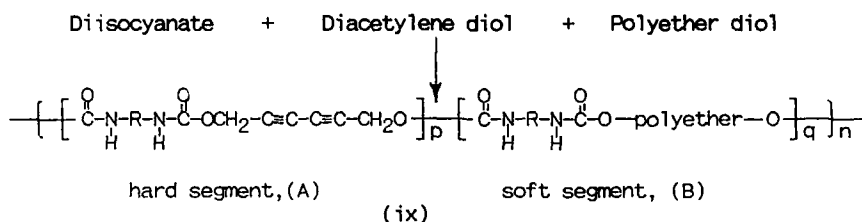


Figure 11. Schematic representation of the formation of segmented urethane-diacetylene copolymers.

of structure (ix) are linear with the soft segment being totally amorphous and the hard segment having some potential for crystallisation. The microstructural features, which define the morphology of such materials, are shown schematically in fig 12 and in the case of PPG/HDD/MDI copolymers, the thin lines represent the polyoxypropylene soft segment chains and the sequences of circles and squares represent the diacetylene-MDI, hard segment chains. Phase separation results in aggregation of the hard segments into highly hydrogen-bonded, rigid domains. It should be noted that the size and orientation of domains varies, that there is a distribution of hard segment chain lengths and that some isolated hard segments are seen to be dispersed (or phase-mixed) within soft segment chains.

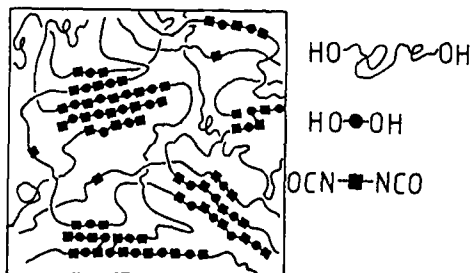


Figure 12. Schematic diagram of the major microstructural features in a segmented urethane-diacetylene copolymer.

As described in the introduction, diacetylene units if present in suitable aggregated form, as either crystallites or complexes, and if subjected to heat or irradiation, undergo topochemical reaction to form the polydiacetylene. In the case of the segmented copolyurethanes with the type of microstructure depicted in fig 12, topochemical reaction proceeds along arrays of diacetylene units attached (or adsorbed) in a spatially, well-defined manner within rigid, hydrogen-bonded hard segment domains dispersed in the soft segment, polyether "solution". This type of reaction is normally referred to as matrix-polymerisation(36) and is clearly an appropriate description in the formation of the present materials since it implies that some information originally present in the template hard segment molecules and domains, such as molar mass and molar mass distribution, type and degree of stereoregularity, is transferred to the reaction product. Thus, assuming the hard segment block in the $(\text{AB})_n$ block copolymer (ix) shown in fig 11 is part of a larger, phase-separated domain, then its structure is transformed by matrix-polymerisation according to the reaction shown in fig 13. (This reaction scheme is analogous to that shown for the formation of EUHD (ii) in the Introduction to Part I of this report, except that the ethyl urethane substituents are now shown as continuing methylenediphenylene urethane chains).

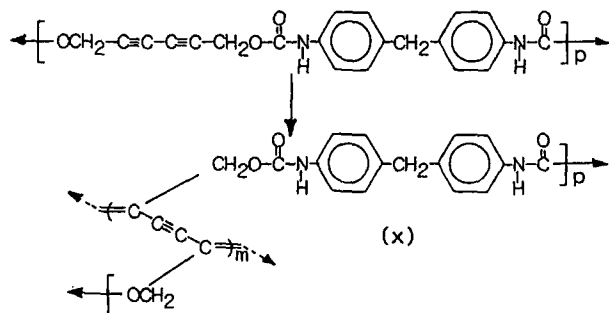


Figure 13. Schematic representation of the topochemical, matrix-polymerisation of diacetylene units to produce cross-polymerised hard segments in urethane-diacetylene copolymers.

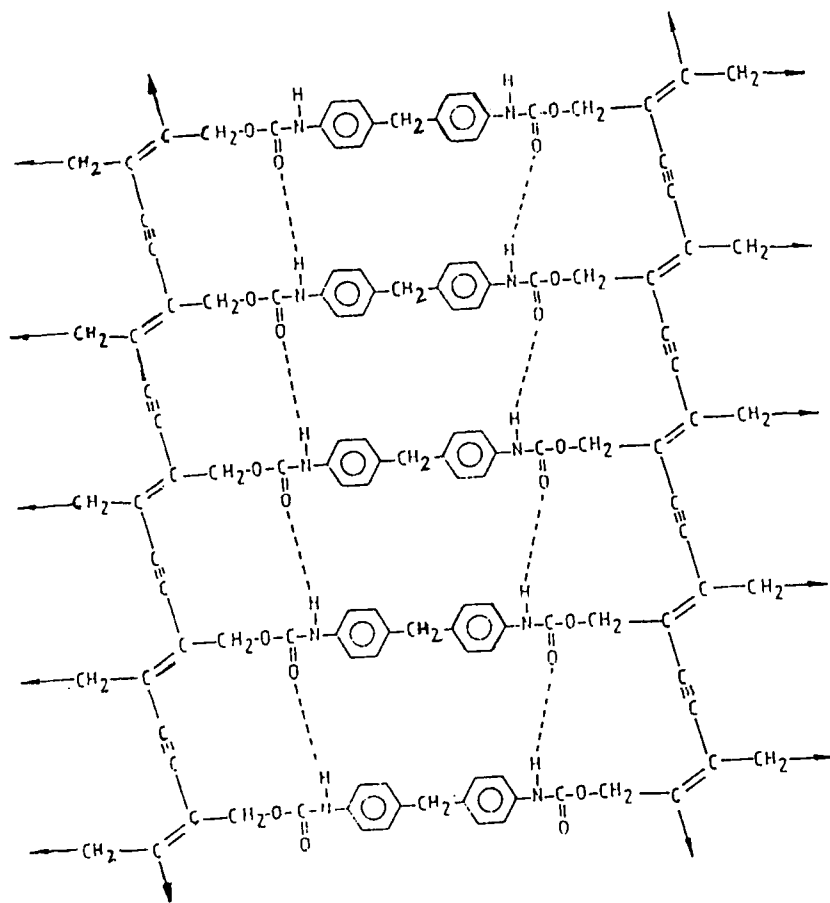


Figure 14. Idealised structure of a cross-polymerised, poly(urethane-diacetylene) hard segment domain showing intermolecular hydrogen bonding between neighbouring urethane groups. The diacetylene chain axis is from top-to-bottom: the methylenediphenylene-urethane chain axis is from side-to-side.

The topochemical, matrix-polymerisation causes a configurational change in specific parts of the hard segments and the resulting chains forming hard segment domains are cross-polymerised. Hard segments thus comprise two different polymer chains whose axes, relative to each other, define different spatial directions. These are depicted schematically in the simplified structure (x) with the polydiacetylene (repeat structure in curved parenthesis, DP = m) shown as a diagonal chain with direction from top left to bottom right, and the methylenediphenylene-based polyurethane (repeat structure in square parentheses, DP = p) as a stepped, horizontal chain. The polydiacetylene chain may be regarded as a polymeric crosslink and the overall crosslink density in the hard segment is therefore very high. The overall three-dimensional structure of the finally cross-polymerised hard segments is shown by the idealised representation in fig 14 which depicts the domain as a completely hydrogen-bonded, ladder polymer. The degree of crosslinking depends on the extent of cross-polymerisation which for a given weight fraction of hard segments, is related to the average degree of polymerisation, p , in structure (x) and to domain size as determined by the degree of phase separation between hard segments and the soft segment matrix.

These urethane-diacetylene copolymers, therefore, are characterised by complex molecular and morphological structures, and the various processes of copolymerisation, phase-separation and topochemical cross-polymerisation occur simultaneously to varying degrees during the materials preparation producing dramatic colour changes and intensification. This is inevitable in a one-step bulk polymerisation process in which a rapid exotherm is produced.

(a) Thermal Properties: Differential Scanning Calorimetry, DSC

DSC measurements were carried out as described in section I.2(d) except that the temperature range used was -100 to 280°C on sample sizes in the range 18 to 22 mg. Typical DSC curves are shown in fig 15(a) - (c) in which curves A refer to partially-reacted and lightly cross-polymerised (orange/brown coloured) materials obtained prior to curing at 120°C for 36 hours. Curves B refer to completely-reacted and more highly, but not fully, cross-polymerised (deep brown/purple coloured) materials. Curves C in fig 15(a) and (b) are for the homopolyurethane soft-segment materials,

PPG1000/MDI and PPG400/MDI, respectively. Curve B' in fig 15(c) is for the homopolyurethane hard segment material, HDD/MDI, which has been quench-cooled from 280 to -100°C after DSC measurement on the same material giving the original curve B. (Note. For clarity, the DSC curves of fig 15(a)-(c) are split into left and right-hand plots which have identical temperature scales but different exothermic-endothemic ordinate scales, with the right-hand plots having the smaller scales.)

The homopolyurethane soft-segment materials show only one transition as an exothermic base line shift, resulting from a glass-to-rubber transition. The corresponding urethane-diacetylene copolymers show similar transitions but there are also pronounced exothermic peaks at much higher temperatures ($>200^{\circ}\text{C}$) attributed to thermally-induced, liquid-phase cross-polymerisation(36). In neither copolyurethane was an exothermic peak(s) observed between 50 and 200°C which might have been expected from melting of hard-segment crystalline domains. The absence of endothermic melting behaviour is probably due to the low molar mass and partial cross-polymerisation of the hard segments in both uncured and cured materials. Even in the isolated, homopolyurethane hard segment material, no evidence of any melting endotherms was observed as shown in fig 15(c), or if there were, the melting temperatures coincided with and were masked by the much more intense cross-polymerisation exotherms. In all cases, the intensity of and the area beneath the exothermic peaks are significantly reduced on curing the materials ($120^{\circ}\text{C}/36\text{h}$) showing increased cross-polymerisation of the hard segments. However, complete cross-polymerisation (or elimination of the exothermic peak) could never be achieved by thermal treatment. In separate experiments, extending the cure time to 48 hours at 120°C produced no further reduction in intensity of the exothermic peak in DSC traces, but did initiate thermal degradation and the material became friable.

An interesting feature in the DSC curves fig 15(c) for HDD/MDI is the development of a glass-transition at 85°C in curve B' following quench-cooling. The ladder-like, hard-segment structure in fig 14 suggests molecular mobility to be severely restricted and would appear to account for the absence of a glass-transition as confirmed by curves A and B. However, after quench-cooling from 280 to -100°C , the hard-segment domain structure is disrupted and hydrogen-bonding reduced sufficiently that relatively large-scale, co-operative segmental motion along chains between

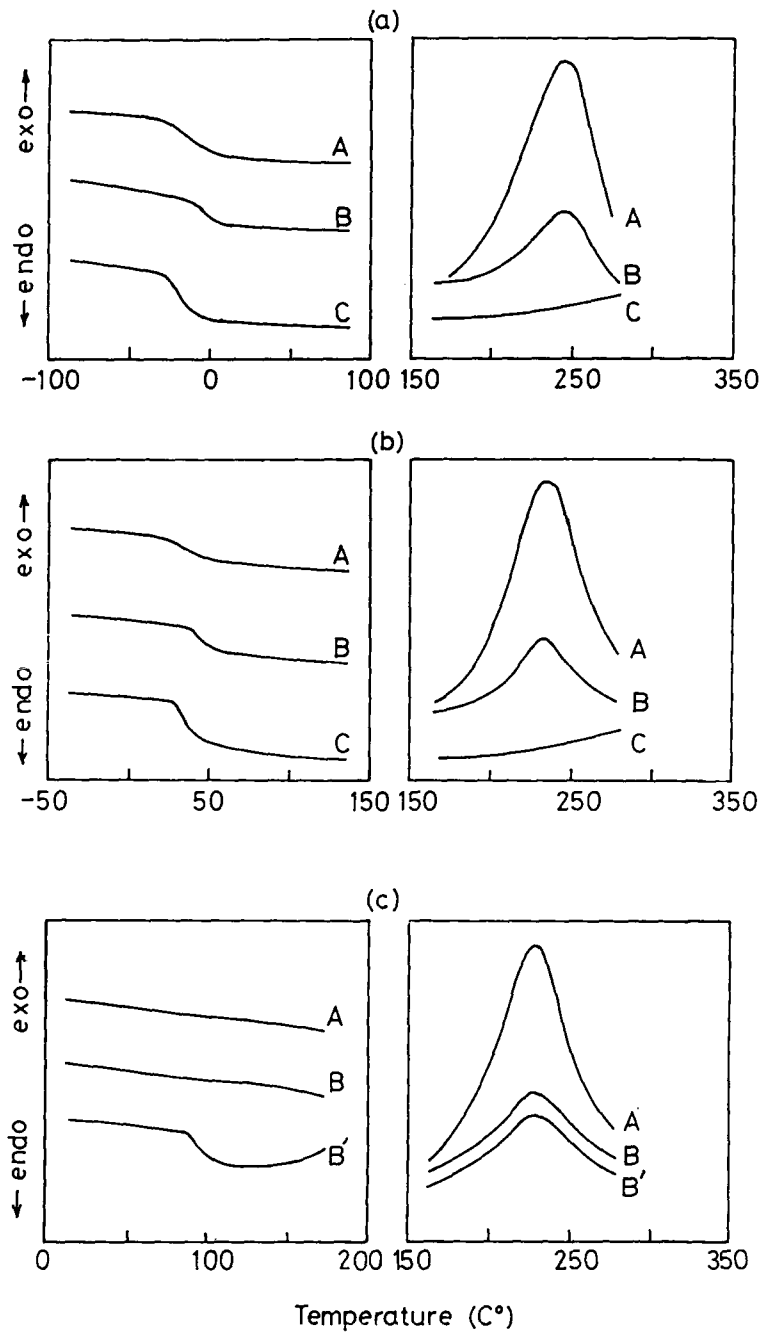


Figure 15. DSC curves for (a) PPG1000-based copolyurethanes (A and B) and homopolyurethane (C); (b) PPG400-based copolyurethanes (A and B) and homopolyurethane (C); (c) HDD/MDI homopolyurethanes (A and B), with curve B' obtained from sample B after quenching (280 to -100°C).

acetylinic crosslinks becomes possible and T_g can be observed at 85°C. The transitional behaviour derived from the various DSC curves is summarised in Table 5 in which T_g refers to the glass-transition temperature, and T_{cp} refers to the cross-polymerisation temperature, determined from the peak value of the exotherm. In the last two columns of Table 5, PSR refers to the phase-separation ratio and is determined(37) as the heat capacity change per unit mass, $\Delta C_p/m$, at T_g for the copolyurethane relative to $\Delta C_p/M$ for the corresponding homopolyurethane soft-segment. For complete phase-separation, PSR = 100%, and for complete phase-mixing, PSR = 0%.

Table 5. Thermal Transitions (DSC) of Homopolyurethanes and Urethane-Diacetylene Copolymers

Material	HS (%)	T_g (a) (°C)	T_g (b) (°C)	T_{cp} (a) (°C)	T_{cp} (b) (°C)	PSR(a) (%)	PSR(b) (%)
PPG1000/MDI	0	-	-28	-	-	-	-
PPG1000/HDD/MDI	22.4	-32	-13	245	248	86	65
PPG400/MDI	0	-	26	-	-	-	-
PPG400/HDD/MDI	33.5	23	37	235	235	89	70
HDD/MDI	100	(c)	85(d)	230	230	-	-

(a)uncured (partially-reacted, lightly cross-polymerised).

(b)cured 120°/36h (completely-reacted, highly cross-polymerised).

(c)not detected.

(d)quench-cooled sample (280 → -100°C).

Values of T_g for PPG1000/MDI and PPG400/MDI (-28 and 26°C) are for homopolyurethane matrices in which complete conversion of -OH and -NCO groups (to urethane) has been achieved. Introducing diacetylene-based hard segments in the uncured copolyurethanes, PPG1000/HDD/MDI and PPG400/HDD/MDI, results in small decreases in T_g (-32 and 23°C). This occurs because in the uncured materials, conversion of -OH groups on PPG to yield higher molar mass poly(ether-urethane) soft-segments is incomplete,

as is the reaction via urethane formation with the developing poly(diacetylene-urethane) hard-segments. Nevertheless, despite incomplete reaction, a significant amount of conversion has occurred since the Tg of totally-unreacted PPG is $\sim 65^{\circ}\text{C}$. Also in the uncured materials, the degree of phase separation is high as indicated by the values of PSR ($>85\%$). The high degree of phase-separation is surprising since the uncured materials were formed at 80°C (increasing to $\sim 120^{\circ}\text{C}$ with the exotherm) which is around Tg of the HDD/MDI hard segment. Under these conditions, hard segment vitrification is delayed and phase-separation is reduced. However, the development of hard segment molar mass (which must be sufficiently high in the first place for vitrification and phase-separation to occur) may be affected by the small amount of cross-polymerisation occurring, which reduces molecular mobility and the ability of hard segment oligomers to further react. Cross-polymerisation may also lead to the formation of hard segment domains with sizes smaller than would otherwise be the case in solely linear systems.

In the cured materials, PPG1000/HDD/MDI and PPG400/HDD/MDI, $-\text{OH}$ and $-\text{NCO}$ reactions are complete. All PPG chains are connected via urethane groups into the soft-segment matrix and to hard-segments whose mean length has been increased. In addition, cross-polymerisation has been maximised (but not completed). During cure ($120^{\circ}\text{C}/36\text{h}$) which is well above hard-segment Tg (85°C), full polyurethane development and the increased crosslinking in the hard-segment phase have caused extensive phase-mixing to occur as shown by the significant reduction ($\sim 20\%$) in PSR values. Consequently, Tg values for the cured copolyurethanes, PPG1000/HDD/MDI and PPG400/HDD/MDI, have increased by 19 and 14°C , respectively, to values well above those for PPG1000/MDI and PPG400/MDI (the isolated soft-segment matrices). Larger effects are observed for the PPG1000-based system, since the longer polyether chains, lower hard-segment content and degree of cross-polymerisation allow greater molecular mobility and easier phase-mixing in the copolyurethane.

Values of T_{cp} in Table 5 show that the maximum rate of topochemical cross-polymerisation in hard segment domains, occurring between 230 and 250° , is not affected by the materials thermal history (during formation or curing). The intensity of the exotherm, however, which is proportional to the concentration of diacetylene units in hard segment domains, is significantly reduced by a factor of three in both copolymers. Thus, given

the higher hard-segment content and phase-separation in PPG400/HDD/MDI, it would appear that the efficiency and degree of cross-polymerisation achieved in these materials are greater for copolyurethanes based on higher molar mass soft segments: that is, PPG1000 compared with PPG400.

(b) Dynamic Mechanical-Thermal Behaviour

Modulus-temperature and mechanical damping-temperature behaviour were obtained over the temperature range -150 to 200°C using the DMTA technique described in Part I of this report. Typical $\log(E')$ and $\tan \delta$ versus temperature plots for the homo- and copolyurethanes based on PPG1000 and PPG400 are shown, respectively, in fig 16-19. Considering first the damping curves, the linear homopolyurethanes, PPG1000/MDI and PPG400/MDI, both show three relaxations which, in order of decreasing temperature are designated α , β and γ . The α -transition is clearly the most intense and is associated with the glass transition of the polymer, located at T_g . The lower intensity peaks, β and γ , are secondary relaxations attributed to molecular motions similar to those discussed in Part I for associated water-urethane complexes and oxypropylene units in polyether-rich domains, respectively. The temperatures and peak intensities of α -, β - and γ -relaxations are summarised in Table 6. The modulus-temperature behaviour

Table 6. Dynamic Mechanical-Thermal Properties of Homopolyurethanes and Urethane-Diacetylene Copolymers

Material	HS (%)	$\alpha(T_g)$ $\tan \delta$ (°C) (max)	β $\tan \delta$ (°C) (max)	γ $\tan \delta$ (°C) (max)
PPG1000/MDI	0	0 0.74	-30(a) 0.02	-68 0.03
PPG1000/HDD/MDI	22.4	25 0.45	- -	-65 0.02
PPG400/MDI	0	45 0.72	-15 0.02	-68 0.03
PPG400/HDD/MDI	33.5	75 0.48	- -	-64 0.02

(a) approximate value: shoulder merged with $\alpha(T_g)$ transition.

for these two homopolyurethanes is similar with the significant reduction in $\log(E')$ occurring at T_g followed by a small rubbery region before

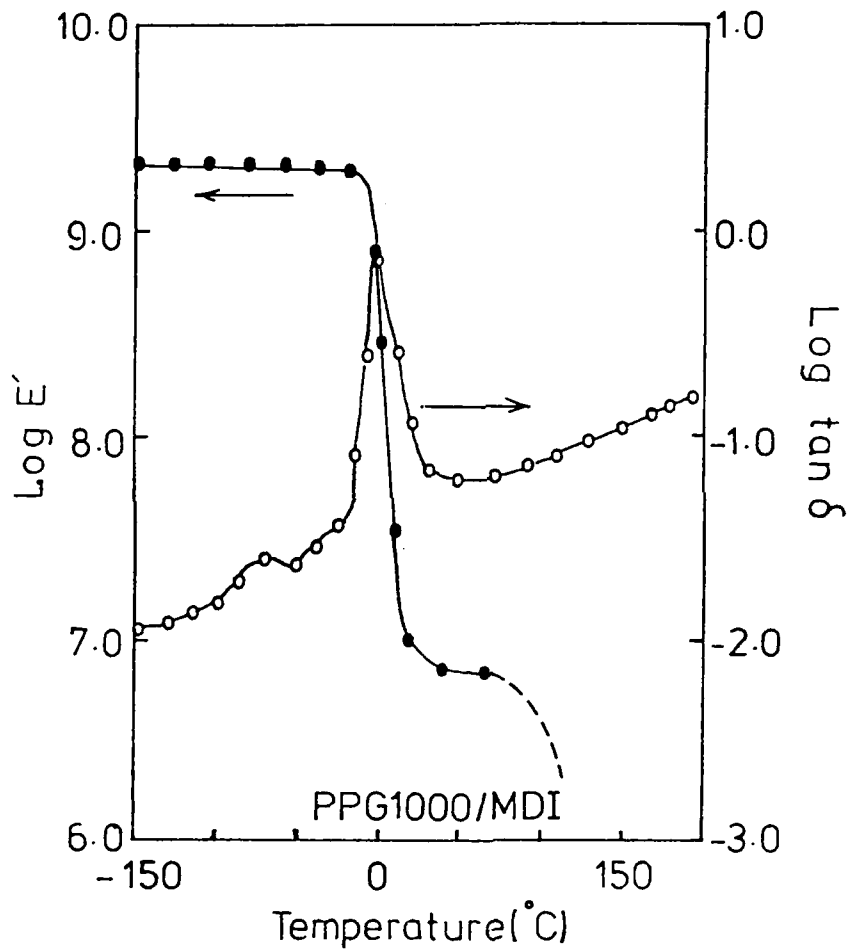


Figure 16. DMTA curves ($1H_z$) for homopolyurethane, PPG1000/MDI, showing storage flexural modulus (E') and mechanical damping ($\tan \delta$) versus temperature.

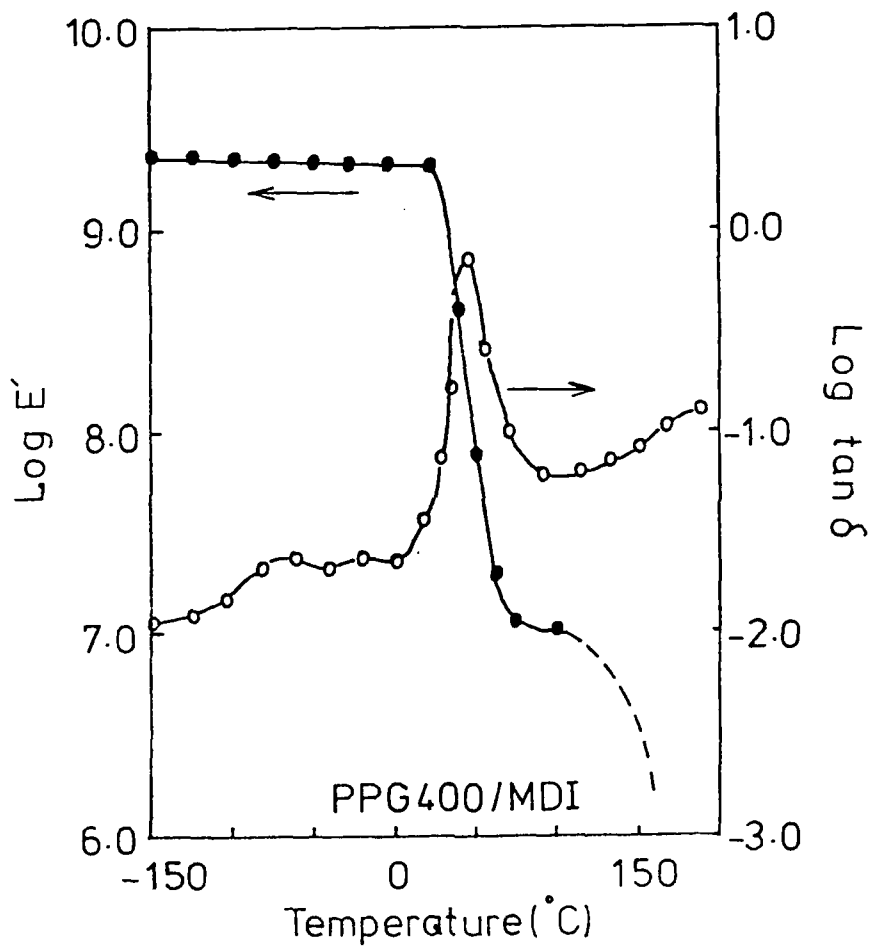


Figure 17. DMTA curves ($1H_z$) for homopolyurethane, PPG400/MDI, showing storage flexural modulus (E') and mechanical damping ($\tan \delta$) versus temperature.

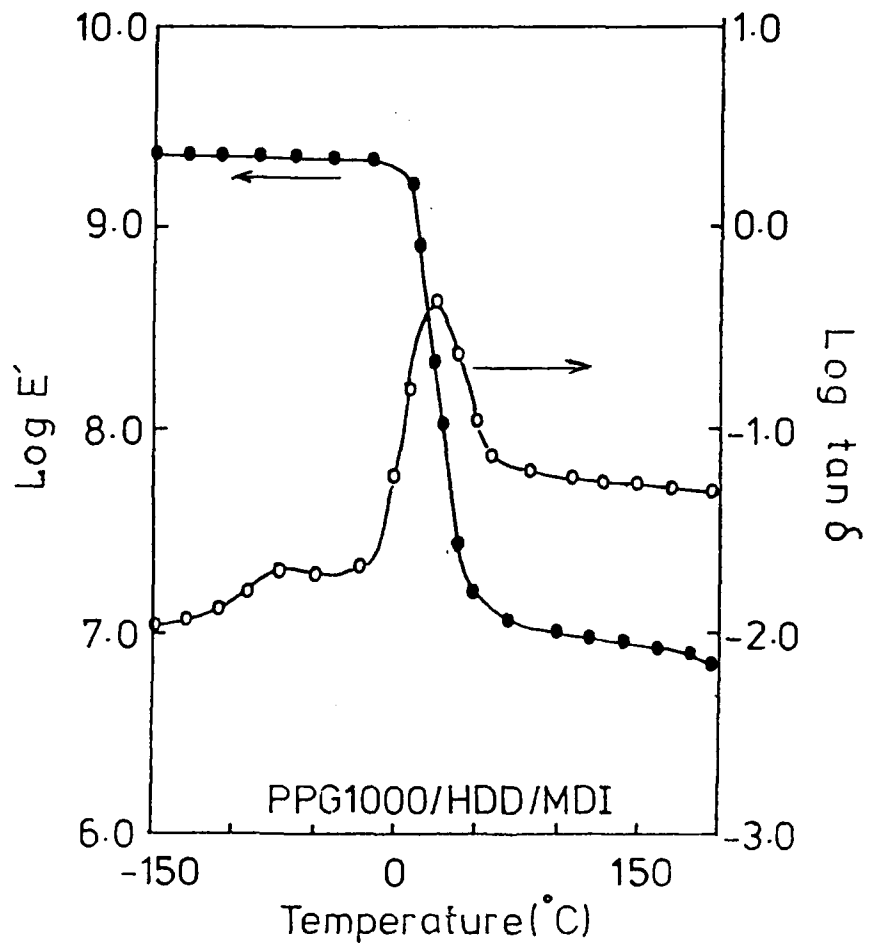


Figure 18. DMTA curves ($1H_z$) for cross-polymerised copolyurethane, PPG1000/HDD/MDI, showing storage flexural modulus (E') and mechanical damping ($\tan \delta$) versus temperature.

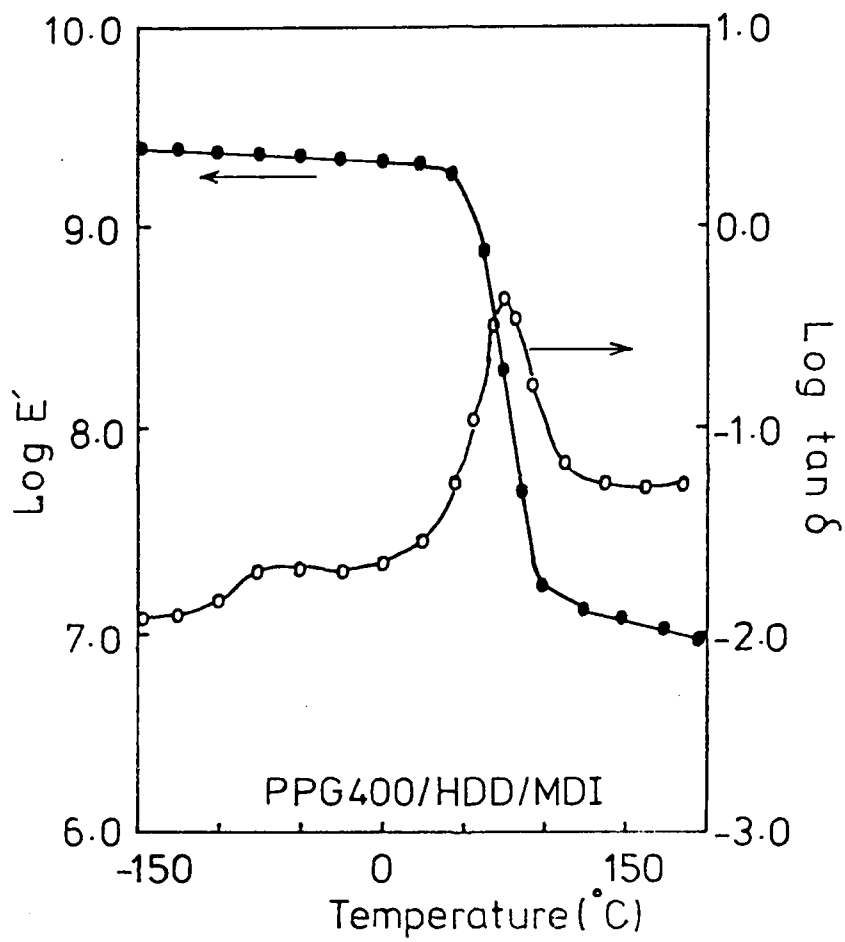


Figure 19. DMTA curves ($1H_z$) for cross-polymerised copolyurethane, PPG400/HDD/MDI, showing storage flexural modulus (E') and mechanical damping ($\tan \delta$) versus temperature.

decreasing rapidly (coinciding with the sharp rise in $\tan \delta$) as the materials transform to the liquid state. The main differences between PPG1000/MDI and PPG400/MDI occur with the location of T_g and the value of rubbery modulus above T_g , both of which are increased as the molar mass of the PPG used in polyurethane formation is decreased (or the relative proportion of aromatic MDI to aliphatic polyether is increased).

Incorporating cross-polymerised, urethane-diacetylene hard segments into both materials results in significant increases in $\log E'$ and reductions in $\tan \delta$ as functions of temperature, as seen in fig 18 and 19 for PPG1000/HDD/MDI and PPG400/HDD/MDI. Most notable is the 25 to 30°C rise in T_g (see footnote) and the corresponding 30 to 40% decrease in the peak value of $\tan \delta$ (as well as the broadening of the peak). These changes are due to the phase-mixing between polyether soft segments and poly(urethane-diacetylene) hard segments, as indicated previously by the values of PSR in the final column of Table 5. On the basis of the footnote and the value of T_g (85°C by DSC) reported in Table 5 for HDD/MDI, the value of T_g by DMTA for the isolated hard-segment would be expected to be between 110 and 115°C. The closer proximity of T_g for PPG400/HDD/MDI to that of HDD/MDI, compared with PPG1000/HDD/MDI, is directly attributed to the higher hard-segment content of the former copolymer. The damping curves for the copolymers also show that the β -peak has disappeared, which is presumably due to reduced moisture adsorption, compared with the homopolyurethanes. In addition, there is a small, but noticeable increase in temperature location of the γ -peak (from -68 to -64°C) and a corresponding reduction in the peak value of $\tan \delta$ (0.03 to 0.02) for the copolymer. This again confirms that phase-mixing has occurred during cross-polymerisation of these materials.

The biggest effects on modulus-temperature behaviour of incorporating cross-polymerised, hard-segments is observed above T_g by the higher values of $\log E'$ and the extended rubbery modulus plateau (coinciding with the

Footnote: T_g values in Table 6 correspond to the T_g values in the second column of Table 5 (DSC). The 20 to 40°C differences in T_g values is attributed to differences in DSC and DMTA techniques and the analysis methods used to determine T_g from experimental data

steady level of damping in this temperature region). The dynamic mechanical-thermal data clearly show that the otherwise linear homopolyurethanes are transformed into non-linear, copolyurethanes with improved modulus- and damping-temperature behaviour. The copolymer materials are characterised by intermediate degrees of phase-separation and by crosslinking which is due entirely to cross-polymerised, polyurethane-diacetylene hard segments.

(c) Tensile stress-Strain Properties

Tensile measurements were carried out at 23°C using dumb-bell specimens of gauge length 30 mm and an extension rate of 1 mm min⁻¹. Average stress-strain curves are shown in fig 20 for PPG1000/MDI and PPG1000/HDD/MDI, and in fig 21 for PPG400/MDI and PPG400/HDD/MDI. Tensile properties derived from these curves are summarised in Table 7 in which the various symbols have already been defined in Part I of this report.

Table 7. Tensile Properties of Homopolyurethanes and Urethane-Diacetylene Copolymers.

Material	HS (%)	E (MPa)	σ_u (MPa)	ϵ_u (%)	U_t (MJ m ⁻³)
PPG1000/MDI	0	0.8	0.57	280	0.001
PPG1000/HDD/MDI	22.4	15.8	8.35	165	0.009
PPG400/MDI	0	482	20.32	4.0	1.503
PPG400/HDD/MDI	33.5	1594	67.65	2.2	2.423

The linear homopolyurethane, PPG1000/MDI, has a T_g of 0°C (DMTA) and at room temperature, therefore, behaves as a very soft, weak and friable elastomer. Incorporating only 22.4% w/w of hard segments increases stiffness and strength by factors of ~20 and 15, respectively, whilst only halving ultimate elongation. Consequently, copolymer PPG1000/HDD/MDI is

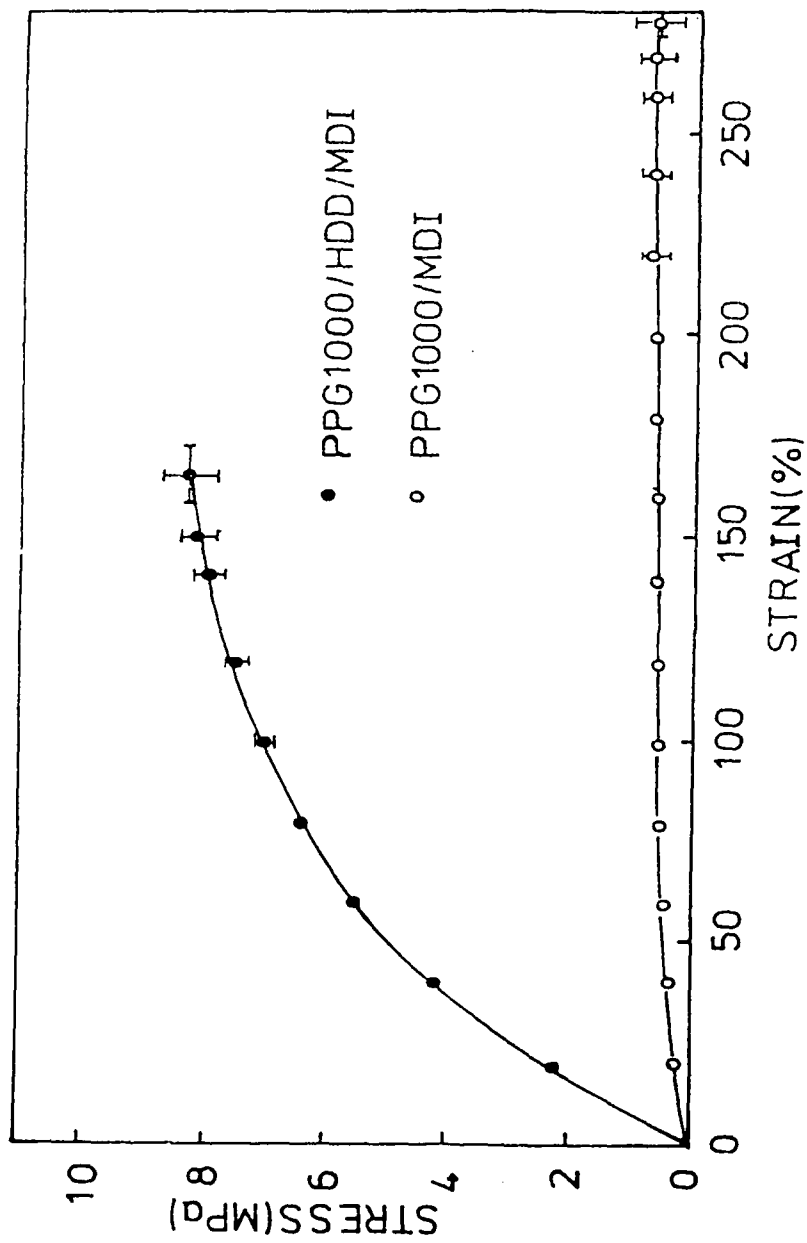


Figure 20. Tensile stress-strain curves (23°C) for PPG1000-based homopolyurethane and cross-polymerised, urethane-diacetylene copolymer.

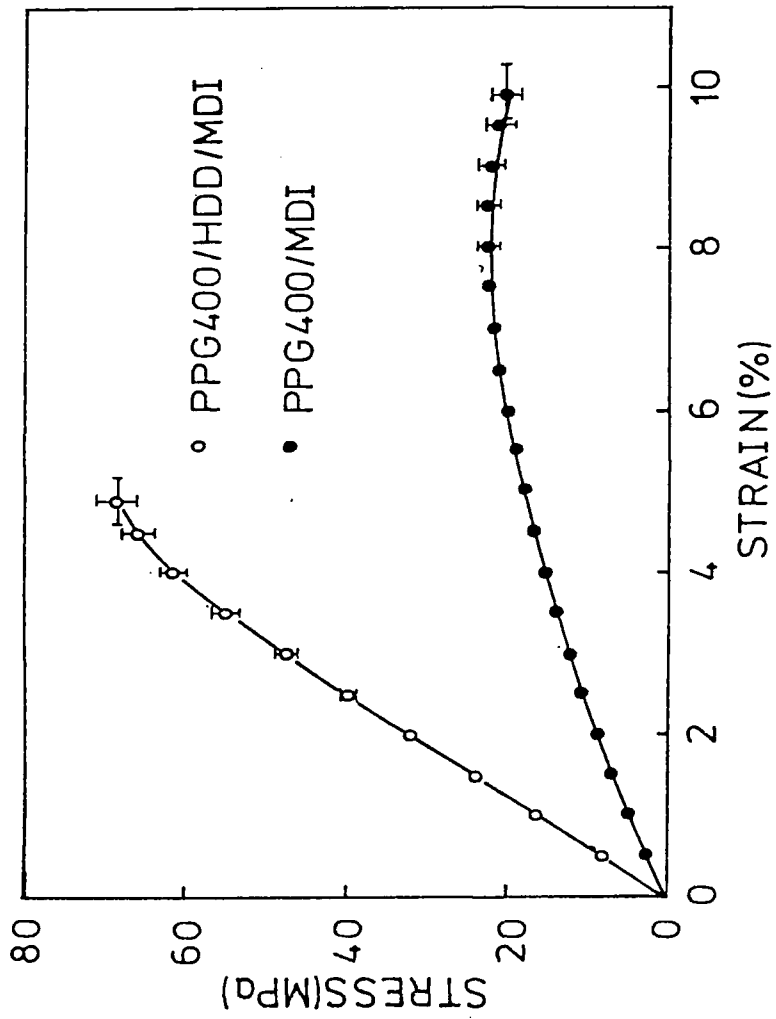


Figure 21. Tensile stress-strain curves (23°C) for PPG400-based homopolyurethane and cross-polymerised, urethane-diacetylene copolymer.

nearly an order of magnitude tougher. This transformation in mechanical behaviour arises from both the upward shift in T_g to 25°C and the reinforcing effects resulting from the stiff, highly-crosslinked poly(urethane-diacetylene) hard segments. In the case of PPG400/MDI, which has a T_g of 45°C (DMTA), the material exhibits the "leather-like" characteristics of a linear polymer in its transition region; that is, an intermediate value of modulus (10^8 - 10^9 Pa) and ductile deformation behaviour with slight evidence of yielding (see bottom curve of fig 21). Incorporating a higher level of hard segments (33.5% w/w), however, produces less dramatic changes in relative terms, compared with PPG1000/MDI. Nevertheless, the copolymer PPG400/HDD/MDI is transformed into a strong, glassy and tougher material. The significant upward shifts in T_g to 75°C and the reinforcing effects of the cross-polymerised hard-segments again account for these changes in tensile properties.

These limited tensile data do show significant differences in the reinforcing efficiency of cross-polymerised hard segments on otherwise soft and weak poly(ether-urethane) matrices, despite the small variations in hard-segment content and degree of phase-separation. Clearly, a more sophisticated technique giving greater detailed analysis is required to examine localised stresses and strains, and even their distributions between the different phases, in relation to the gross deformation of these types of copolymer materials. Such a technique is afforded by Raman spectroscopy, which has been used to investigate the micromechanics of deformation in these materials and is described in the following sections.

II.4 Deformation Micromechanics of Urethane-Diacetylene Copolymers using Raman Spectroscopy.

(a) Raman Spectroscopy: Experimental.

Raman spectra were obtained from cross-polymerised samples using a Raman microscope system. This is based upon a SPEX 1403 double monochromator connected to a modified Nikon optical microscope. Spectra were obtained at a resolution of the order of ± 5 cm^{-1} using the 632.8 nm line of a 10 MW He/Ne laser. A x40 objective lens with a numerical aperture of 0.65 was employed and this gave a 2 μm spot when focussed (although the objective lens was generally de-focussed to reduce the possibility of damage through excessive heating). In the case of deformed

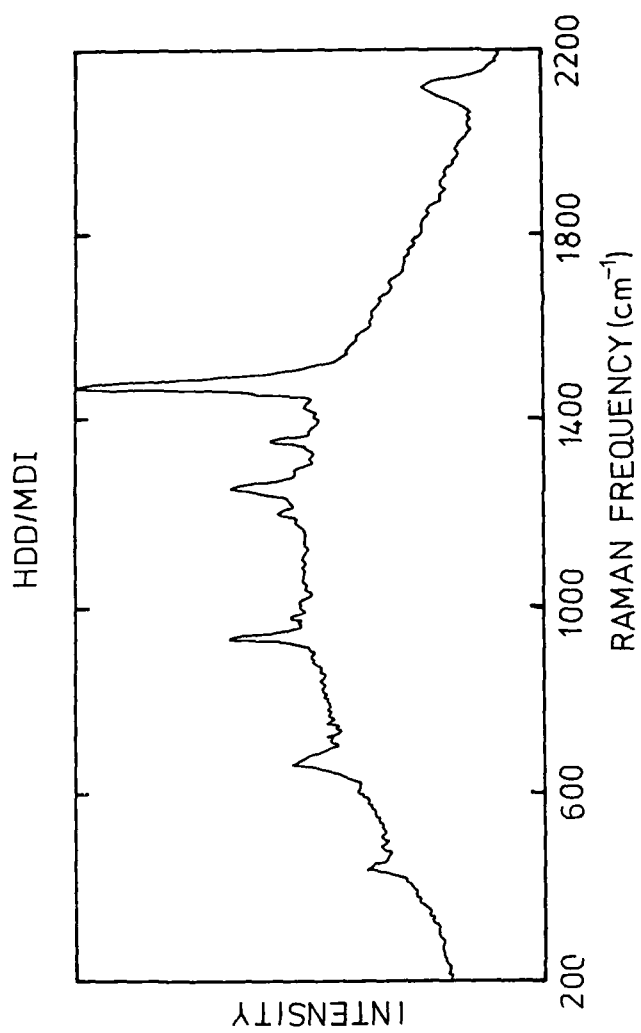


Figure 22(a). Raman Spectrum of HDD/MDI obtained in the range 200cm^{-1} to 2200cm^{-1} .

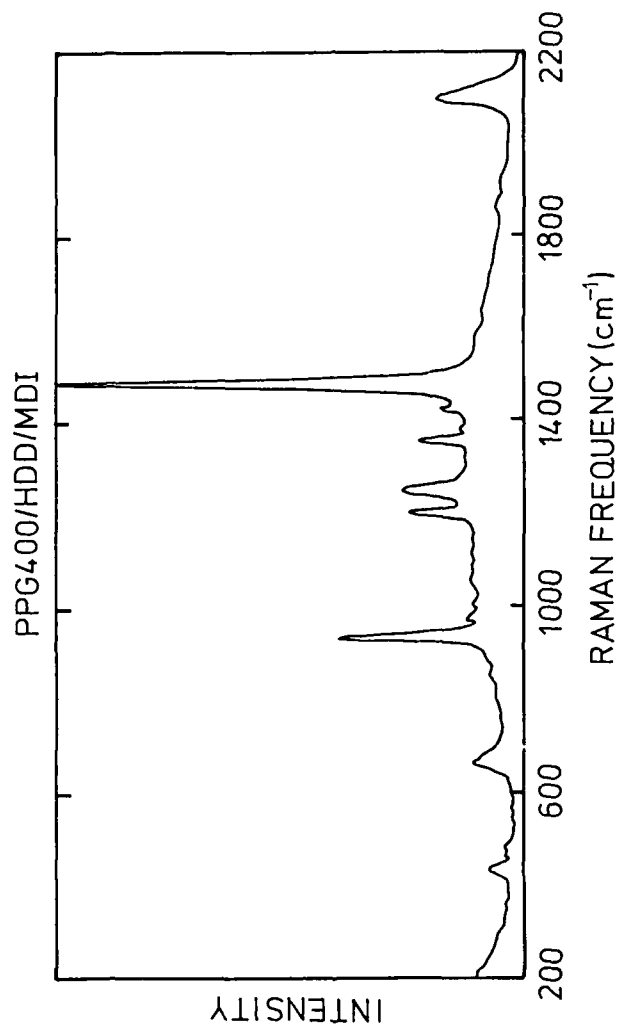


Figure 22(b). Raman Spectrum of PPG400/HDD/MDI obtained in the range 200cm^{-1} to 2200cm^{-1} .

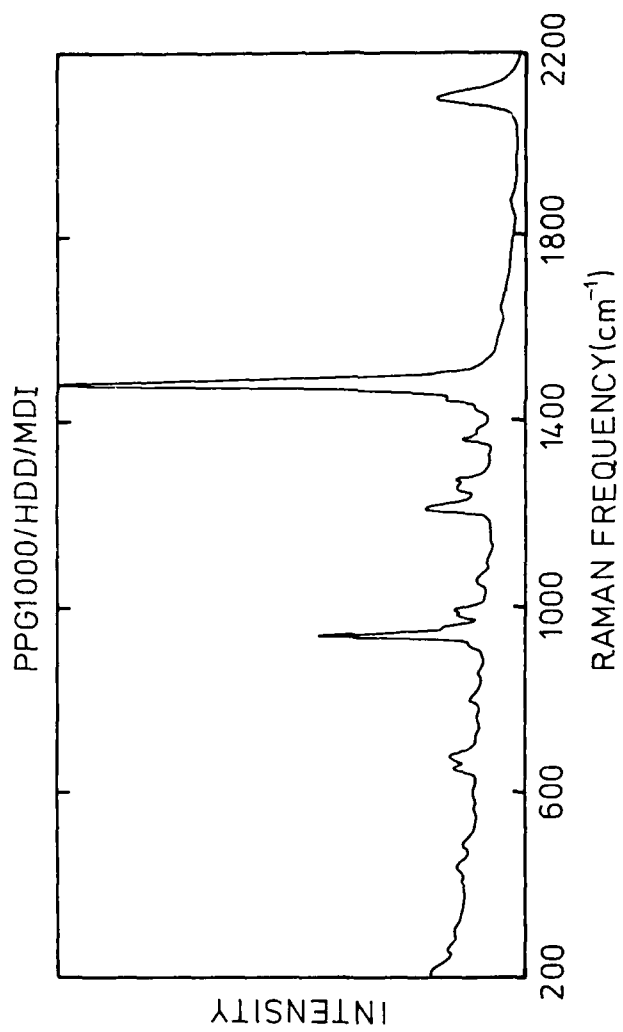


Figure 22(c). Raman Spectrum of PPG1000/HDD/MDI obtained in the range 200cm^{-1} to 2200cm^{-1} .

samples, the laser beam was always polarised parallel to the tensile axis.

Spectra were obtained from the surface strips of cross-polymerised material, approximately 2 x 10 x 50 mm, during deformation using a Polymer Laboratories "Mini-mat" mechanical testing machine. This is designed specifically to fit onto the stage of an optical microscope. The strips were deformed to fixed displacements using a gauge length of the order of 30 mm. The strain was determined from the gauge length and the displacement. The load on the specimen was also monitored using a 200N load cell. Each spectrum was determined over a period of about 10 minutes. It was found that stress relaxation took place during deformation over this period of time and the stresses quoted are mean values.

(b) Analysis and Discussion of Raman Spectra

It was found that Raman spectroscopy could be used to obtain spectra from cross-polymerised samples of the copolymers. Figure 22 shows a series of spectra for the HDD/MDI pure hard segment (fig 22a), the PPG400/HDD/MDI glass (fig 22b) and the PPG1000/HDD/MDI elastomer (fig 22c). A broad fluorescent background was obtained for the HDD/MDI hard segment but this was found to decrease between fig 22a and 22c with the incorporation of the PPG soft segment and as the length of the soft segment increased. This was probably due to both an increase in order and a reduction in the proportion of MDI aromatic groups. The spectra are similar to those obtained by Rubner(29) for his radiation-polymerised, polyurethane-diacetylene copolymers. The spectra in fig 22 contain Raman bands at 1450 cm^{-1} and 2100 cm^{-1} which are characteristic of the double and triple bond vibrations of the conjugated backbone of the diacetylene units(30). The variations between the Raman spectra depend upon coupling of the motion of the side group atoms with that of the backbone atoms. It can be seen that there are some slight differences in the spectra below 1400 cm^{-1} due probably to local variations in the flexibility of side group structures. However, the two main peaks of interest at 1450 cm^{-1} and 2100 cm^{-1} are essentially identical.

One of the main aims of this study was to determine the effect of deformation upon the position of the $\text{-C}\equiv\text{C-}$ triple bond stretching band in the glass and elastomer. It was found that for both materials subjected to an applied tensile strain, the position of the band shifted to lower

frequency as can be seen in fig 23(a) for the PPG400/HDD/MDI glass and in fig 23(b) for the PPG1000/HDD/MDI elastomer. In both cases there is a significant decrease in the peak frequency of the Raman bond coupled with the broadening of the band.

The effect of deformation upon the peak position is shown in more detail for the PPG400/HDD/MDI glass in fig 24. The effect of applied strain is shown in fig 24(a) and that of applied stress in fig 24(b). In both cases there is a linear shift and the rates of shift are listed in Table 8. It should be noted that the value of Young's modulus determined from the data in fig 24 is significantly lower than that obtained from fig 21. This is because the deformation of the material is rather strain-rate sensitive due to the proximity of the T_g (Table 6). The effective strain rate for fig 24 is several orders of magnitude less than that used in fig 21.

The effect of deformation upon the peak position for the PPG1000/HDD/MDI elastomer is shown in fig 25. In this case significantly higher strains could be applied because of the higher elongations possible for the elastomer (fig 20). It can be seen from fig 25(a) that there is a significant decrease in the Raman frequency, $\Delta\nu$, with applied strain but that the change is not linear. On the other hand, the shift in $\Delta\nu$ with applied stress shown in fig 25(b) is found to be linear within the bounds of experimental error. The significance of this behaviour will be discussed later.

The shifts in the Raman bands with deformation was found to be reversible and there was found to be a shift to high frequency when the stress and strain were decreased. This behaviour is shown in fig 26 for the PPG1000/HDD/MDI elastomer. Another point to note from this figure is that when the elastomer is subjected to high degrees of deformation ($\epsilon > 50\%$) multiple peaks are obtained in the Raman spectrum. It can be seen that the band for triple bond stretching in fig 26 shows several peaks when the material is deformed to a strain of 60%. This is indicative of significant local variations in stress and strain in the hard segments. It follows a gradual broadening of the Raman band with increasing deformation and could be due to break-up of the hard segments.

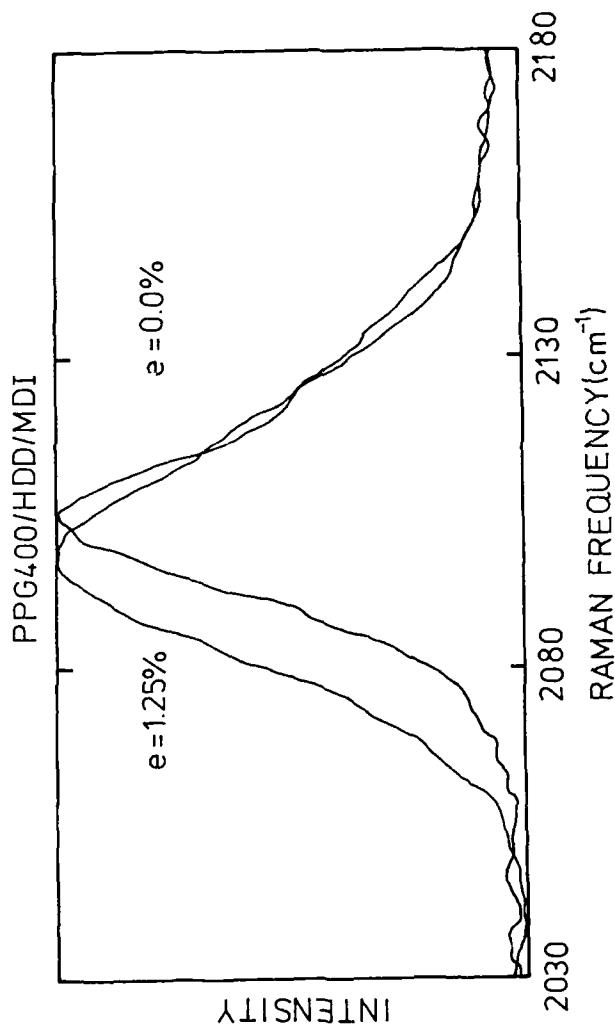


Figure 23(a). Raman spectra of PPG400/HDD/MDI in the region of 2100cm⁻¹ before and after deformation.

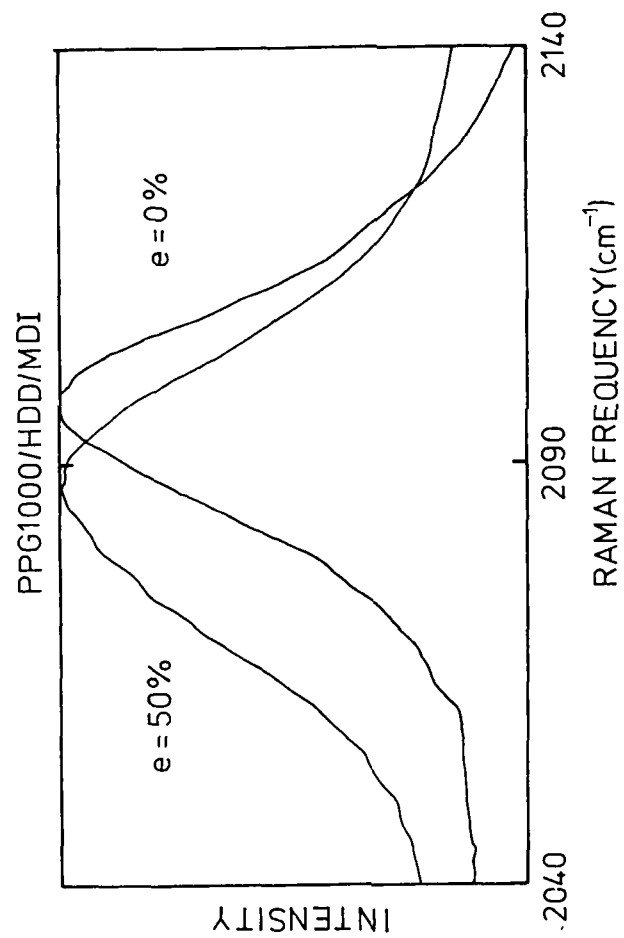


Figure 23(b). Raman spectra of PPG1000/HDD/MDI in the region of 2100cm⁻¹ before and after deformation.

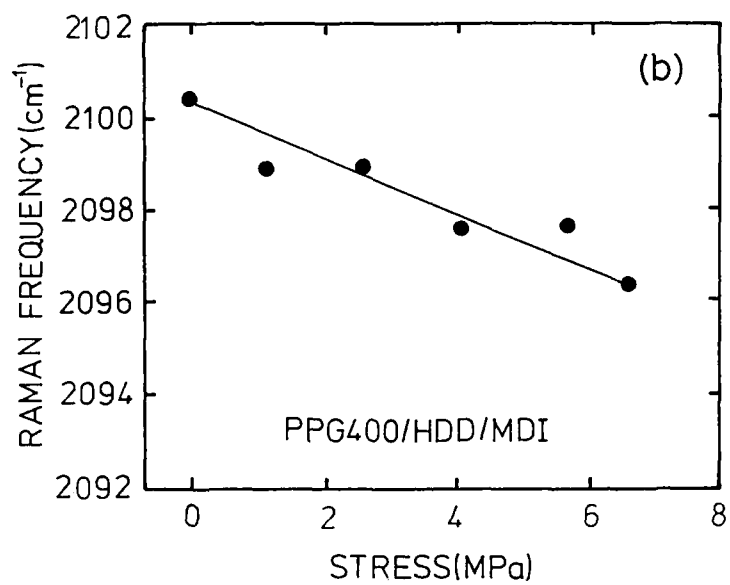
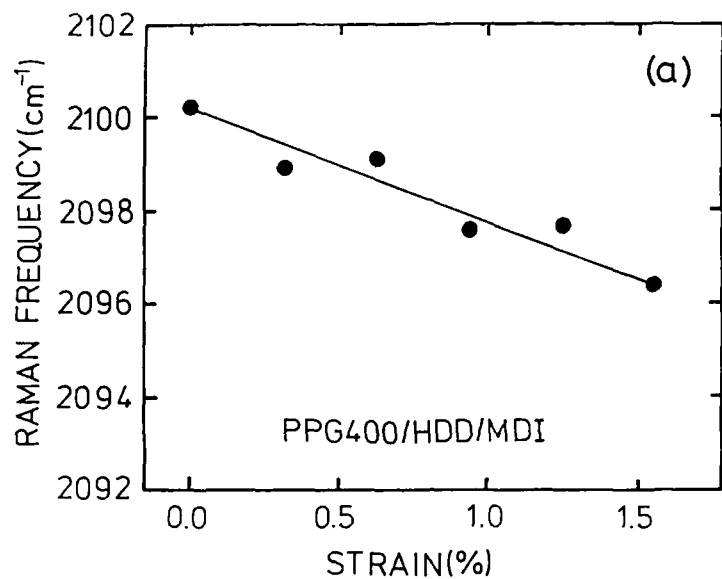


Figure 24. Variation of the position of the 2100cm^{-1} peak in PPG400/HDD/MDI with Deformation
 a) Dependence upon strain
 b) Dependence upon stress.

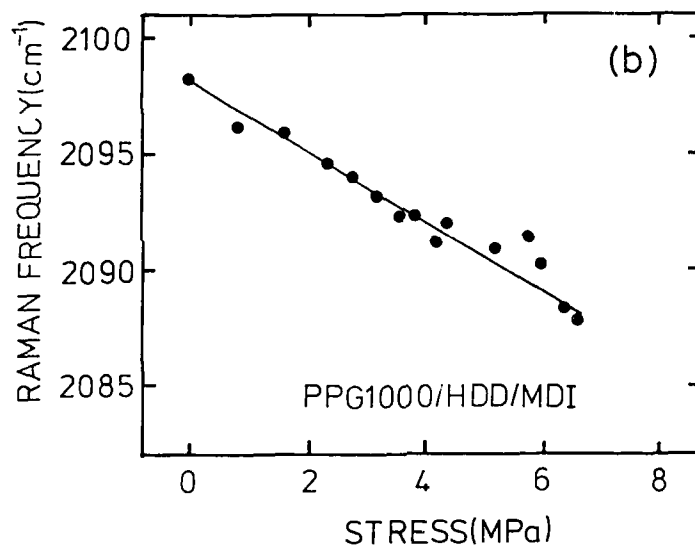
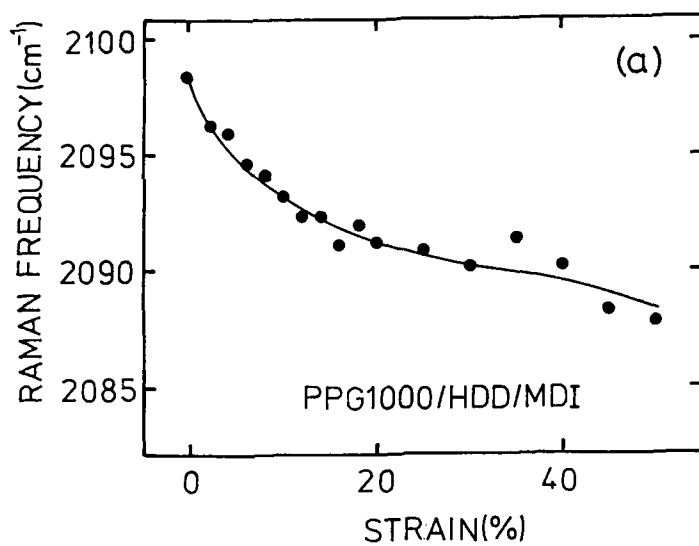


Figure 25. Variation of the position of the 2100cm^{-1} peak in PPG1000/HDD/MDI with Deformation
 a) Dependence upon strain
 b) Dependence upon stress.

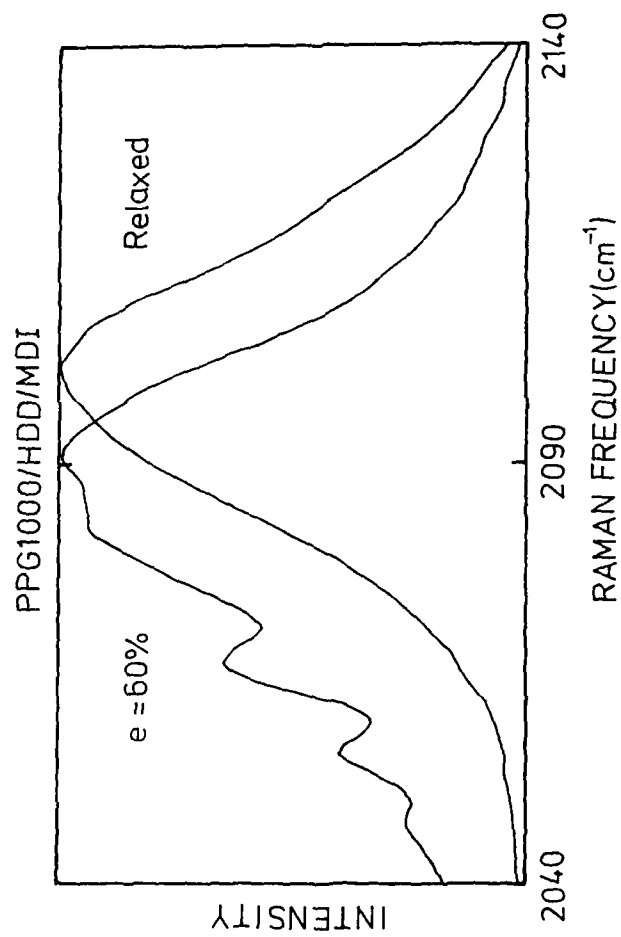


Figure 26. Raman Spectra of PPG1000/HDD/MDI in the region of 2100cm⁻¹ before and after deformation to a strain of 60%, showing break-up of the peak.

Table 8. The Effect of Deformation upon the Peak Frequency, $\Delta\nu$, 2100 cm^{-1} Triple Bond Stretching Band for the Cross-polymerised Polyurethane-diacetylene Copolymers.

Copolymer	$d\Delta\nu/d\varepsilon$ ($\text{cm}^{-1}/\%$)	$d\Delta\nu/d\sigma$ ($\text{cm}^{-1}/\text{MPa}$)
PPG400/HDD/MDI	2.5	0.54
PPG1000/HDD/MDI	0.5(a)	1.53

(a) initial value.

References

1. Cawse, J.L. and Stanford, J.L., Polymer **28**, 356 (1987).
2. Barksby, N., Dunn, D., Kaye, A., Stanford, J.L. and Stepto, R.F.T., in "Reaction Injection Moulding", (ed. J.E. Kresta), ACS Symp. Ser. **270**, ACS, Washington DC, **83** (1985).
3. Day, R.J., Robinson, I.M., Zakikhani, M. and Young, R.J., Polymer **28**, 1833 (1987).
4. Robinson, I.M., Zakikhani, M., Day, R.J. and Young, R.J., J. Mater. Sci. Lett. **6**, 1212 (1987).
5. Chamis, C.C., Hanson, M.P. and Serafini, T.T., NASA Tech. Note D-6463, (August 1971).
6. Hancox, N.L., Composites, **2**, 41 (1971).
7. Hancox, N.L. and Wells, H., Composites, **3**, 26 (1973).
8. Ellis, C.D. and Harris, B.J., Compos. Mater., **7**, 76 (1973).
9. Hull, D., in "An Introduction to Composite Materials", Cambridge University Press, 1981.
10. Ladizesky, N.H. and Ward, I.M., paper presented at 6th International Conference, "Yield, Deformation and Fracture of Polymers", Plastics and Rubber Institute, Cambridge, 1985.
11. Greenwood, J.H. and Rose, P.G., J. Mater. Sci., **9**, 809 (1974).
12. Robinson, I.M., Young, P.H.J., Galiotis, C., Young, R.J. and Batchelder, D.N., to be published.
13. Galiotis, C., Yeung, P.H.J., Young, R.J. and Batchelder, D.N., J. Mater. Sci., **19**, 3640 (1984).
14. Robinson, I.M., Galiotis, C., Young, R.J. and Batchelder, D.N., J. Mater. Sci., **22**, 3642 (1987).
15. Galiotis, C., Young, R.J., Ando, D.J. and Bloor, D., Makromol. Chem., **184**, 1083 (1983).
16. Wegner, G., Z. Naturforsch. Teil B., 824 (1969).
17. Wegner, G., Makromol. Chem. **145**, 85 (1971).
18. Wegner, G., Makromol. Chem. **154**, 35 (1972).
19. Ryan, A.J., Stanford, J.L. and Still, R.H., Br. Polym. J., **20**, 1 (1987).
20. Plati, E. and Williams, J.G., Polym. Eng. Sci., **15**(6), 470 (1972).
21. Phillips, D.C., Scott, J.M. and Jones, M., J. Mater. Sci., **11**, 718, (1979).

22. Yamini, S. and Young R.J., J. Mater. Sci., 15, 1823, (1980).
23. Van Bogart, J.W.C., Lilaonitkul, A. and Cooper, S.L., Adv. Chem. Ser., 176, 3 (1979).
24. Seymour, R.W., Estes, G.M. and Cooper S.L., Macromolecules, 3, 579 (1970).
25. Seymour, R.W., Allegrezza, A.E. and Cooper, S.L., Macromolecules, 6, 896 (1973).
26. Seymour, R.W. and Cooper, S.L., Rubber Chem. Tech., 47, 19 (1974).
27. Rubner, M.F., Polym. Mat. Sci. Eng., 53, 683 (1985).
28. Liang, R.C. and Reiser, A., Polym. Prepr. (Am. Chem. Soc., Div. Polym. Chem.), 26(2), 327, (1985).
29. Rubner, M.F., Macromolecules, 19, 2114 (1986).
30. Batchelder, D.N. and Bloor, D., J. Polym. Sci., Polym. Phys. Ed., 17, 569 (1979).
31. Galiotis, C., Young, R.J. and Batchelder, D.N., J. Polym. Sci., Polym. Phys. Ed., 21, 2483 (1983).
32. Young, R.J., Ch.1 in "Development in Oriented Polymers - 2" (ed I.M. Ward), Applied Science, London, 1987.
33. Aldrich Chem. Co. Ltd., "Catalogue of Fine Chemicals", (1987).
34. Sorenson, W.R. and Campbell, T.W., "Preparative Methods of Polymer Chemistry", Interscience, New York, 1961.
35. Hay, A.S., Org. Chem., 27, 3320, (1962).
36. Wegner, G., Pure & Appl. Chem., 49, 443, (1977).
37. Camberlin, Y. and Pascault, J.P., J. Polym. Sci. Polym. Chem. Edn., 21, 415, (1983).